A PREDICTIVE TORQUE DEMAND CONTROL APPROACH FOR ENERGY MANAGEMENT IN DUAL MOTOR BATTERY ELECTRIC VEHICLE

Author

ADABOH, MARTINS. O

Supervised by

SCIOLA, MARTINA. PhD (MathWorks)
VALENTI, ROBERTO. PhD (MathWorks)
SCARCIOTTI, GIORDANO. PhD

2024

Abstract

Dual motor battery electric vehicle with Independently driven axles have been accepted by the academic community for its dynamic characteristics and potential to improve the energy efficiency of modern purely electric vehicles. However, this will require a more complex energy management system (EMS) especially because of the increased degree of freedom compared to single motor driven power train.

In this paper, focus is given on the use of model predictive control techniques to optimize the dual motor battery electric drive train in torque control mode. A nonlinear model predictive control problem is formulated by a quadratic cost term subject to affine constraint. Proper consideration was given to the discretization technique used for this system which can be classified as moderate to highly stiff due to relatively different time varying dynamics of the vehicle, batteries and motors. This resulted in energy performance improvement for urban drive cycles when the power split ratio between the two electric motors was 50:50. To further improve the algorithm performance, a rule-based logic was implemented to allow the propulsion and braking by the rear and front motors respectively, until a certain threshold beyond which a 50:50 torque split between the motors is used. This resulted in further savings for both urban and highway drive cycles. Driving scenarios with frequent stops generated the most energy savings compared to constant speed drive cycles. Further research could incorporate driving mode selection into the control problem.

Declaration of Originality

I hereby declare that the work presented in this thesis is my own unless otherwise stated. To the best of my knowledge the work is original, and ideas developed in collaboration with others have been appropriately referenced.

Copyright Declaration

Acknowledgements

I wish to express my profound gratitude to the Petroleum Trust Development Fund (PTDF) for their sponsorship. I would not have been able to fund my tuition and expenses otherwise.

Special thanks to my Supervisors: Sciola Martina. PhD (MathWorks), Valenti Roberto. PhD (MathWorks) and Giordano Scarciotti. PhD (Imperial College London) for their invaluable support without which I would not have been able to complete this research project. They answered all my questions and provided very useful feedback during this project.

Table of Contents

List of Acronyms

EV	- Electric Vehicle
MPC	– Model Predictive Control
RB	– Rule-based
OB	- Optimization-based
ICE	- Internal Combustion Engine
DM-BEV	– Dual Motor Battery Electric Vehicle
HEV	– Hybrid Electric Vehicle
BEV	– Battery Electric Vehicle
ECMS	– Equivalent Consumption Minimization Strategy
EMS	– Energy Management System
HWFET	– Highway Fuel Economy Test
WLTP	- World Harmonized Light Vehicle Test Procedure
FTP75	**-** Federal Test Procedure 75
PSO	– Particle Swarm Optimization
IDA	– Independently Driven Axles
IPM	– Interior Permanent Magnet
LPV	– Linear Parameter Varying
MPGe	– Mile per Gallon Equivalent

List of Figures

List of Tables

1

CHAPTER ONE: INTRODUCTION

Contents

1.1 Motivation

According to Ladislaw, Albanese, Fitzgerald & Meckling, 2019, Energy management in electric vehicles (EV) is becoming increasingly important and has been attracting a lot of interest from many in academia and industry. This is due to the proliferation of stringent carbon emission regulations by several countries to curb the negative trend of environmental degradation by improving energy efficiency. BEVs (Battery Electric Vehicles) compared to HEVs (Hybrid Electric Vehicles), and other conventional vehicles offer great opportunity for reductions in the carbon emission(*Electric Vehicles: The Future of Development and Deployment*, 2019)

Beside the above benefits, it is popular knowledge that Electric vehicles are about three times more efficient compared to conventional vehicles (ICE), have higher range of possible

travelling speed, makes little to no noise and have fifty times a smaller number of moving parts. Despite all these benefits, EVs still suffer from having a relatively lower range compared to ICE and its hybrid counterparts. This has provided justification for a lot of research into improving efficiency of this class of EVs to provide a sustainable solution to the problem of range anxiety experienced by modern users (*Overview of Electric Vehicles in India*, 2020).

Some researchers have proposed the dual motor battery electric vehicle in the search for more efficient powertrain architecture. The dual motor BEV configuration makes it possible for more efficient energy use in electric vehicles by enabling an extra degree of freedom and independent control of the two electric motors which make up the powertrain. It is worth mentioning that the low manufacturing cost of BEVs and its simplistic design also does not add any extra layer of complexity compared to the single motor drivetrain(Zheng, Tian & Zhang, 2020). Hence making BEVs a suitable choice and justifying the current attention it has been receiving to improve its performance.

1.2 Project Contribution

The dynamic properties of the dual motor battery electric vehicle have made it a subject of a lot of research into improving its drive train efficiency. To further pursue this subject, this research project is geared towards the use a modern online multivariable control approach: model predictive control (MPC) to design a controller which reduces energy consumption by improving driving range without degrading the overall vehicle performance of a dual motor battery electric vehicle (BEV).

There have been several efforts from the research community channeled to improving efficiency in electric and hybrid powertrain. Some of the efforts include the use of rule-based, optimization-based and reinforcement learning approaches(Louback et al., 2024). This research focuses on the application of an optimization-based to improve the energy efficiency performance of the dual motor BEV. It also explores the combination of optimization and rule-based approaches to further improve efficiency.

However, the problem at hand is not a trivial one. And it is due to factors such as: difficulty in choosing a simple yet suitable model which adequately approximates the open loop response of the system, complex powertrain and energy flow dynamics, and inherent nonlinearities in the interaction between the powertrain components. Apart from nonlinearities in the vehicle dynamics, one would have to deal with interactions (in electric motors and batteries) which in this project are modelled by look-up tables based on the manufacturers data. There is always the possibility for a tradeoff between low degree of details in the modelling which reduces computational burden and, high degree of details which ensures accuracy but lead to increased computational burden. Considering computational resources and suitability for real time application, detailed modeling is usually sacrificed to reduce computational burden (Yang et al, 2021: Cavanini et al, 2022).

Despite the inherent complexities (associated with the powertrain components, nonlinear constraints on the input bounds and power split ratio and driving mode considerations) associated with developing an Energy management system for dual motor battery electric vehicles, it has shown promises in optimizing the efficiency of electric drive train compared to other techniques, powertrain types and architectures. (Louback et al., 2024)

In this project, a non-linear MPC algorithm and a nonlinear MPC plus rule-based algorithm is designed to reduce energy consumption in a dual motor BEV while tracking the reference speed profile for the HWFET (Highway Fuel Economy Test) and WLTP class 3 (Worldwide Harmonized Light Vehicle Test Procedure) drive cycles. The algorithm was tested and validated on a model based on *MathWorks 2023 Powertrain block set* designed to run on a 10ms fixed time step, to show improvement in energy efficiency performance. Further validations were also carried out with FTP75 (Federal Test Procedure) and US06 standard drive cycles(MathWorks, 2024).

First, A nonlinear MPC algorithm is designed to distribute the torque equally between the two motors. As an attempt to further improve performance, another algorithm is built combining the nonlinear MPC and the rule-based driving mode logic(Zheng, Tian & Zhang, 2020).

Results show that energy can be saved in urban applications, using MPC as a control strategy to distribute the torque between the two electric prime movers in a 50:50 split ratio. Also, a combination of nonlinear MPC algorithm to compute the optimal torque, plus rule-based approach to distribute the torque optimally below a certain threshold. This additional rule-based approach can more efficiently handle difficult nonlinearities taking the burden off the MPC controller. It also further improved tracking and energy efficiency performance in both urban and highway drive cycles.

1.3 Objectives

The main objectives of this project are outlined below as gotten from the MATLAB Simulink Challenge Project hub on GitHub platform:

- Design a nonlinear MPC controller for an IDA-DM-BEV model in *MathWorks' Powertrain Block set* using the *Model Predictive Control toolbox*(MathWorks, 2024b).
- Maximize driving range by improving the energy efficiency performance of the dual motor BEV drivetrain(MathWorks, 2024b).
- Evaluate the performance of the MPC algorithm by integrating it into the model with the HWFET and WLTP class 3 as references(MathWorks, 2024b).
- Demonstrate improvement in performance in terms energy or MPGe (Miles Per Gallon of gasoline-equivalent) compared to the baseline controller(MathWorks, 2024b).
- Validate the controller by showing that the constraints were not violated. Also run your controller on different drive cycles (i.e. FTP75, US06)(MathWorks, 2024b).

1.4 Challenges

One major challenge is choosing a suitable model which approximates the behavior of the system. This is no trivial task as one is often faced with the decision of which part of the dynamics to neglect to get a simple enough model to reduce computational burden.

Secondly, the system under consideration can be classified as a moderately to highly stiff system. To solve numerically, problems which are stiff, proper consideration must be given to the magnitude of the time step used in discretization of the model equations to ensure numerical stability and accuracy. The nature of the system impacts the selection of the

discretization technique and solver used. These must be considered in algorithm development to improve speed of computation and overall, the controller performance(Thomas, 1999).

Thirdly, in many literatures driving mode is a major consideration due to performance concerns. Examples are the work done by Zheng, Tian and Zhang (2020) and He et al (2021). One is faced with the choice of either including this driving mode selection in the MPC structure or outside of it. Including driving mode selection in the MPC structure increases greatly the computational burden and the solver may struggle to find the optimal solution where necessary. Due to the added nonlinearities which driving mode selection would impose on the MPC algorithm, only the latter approach was implemented. Driving mode selection was implemented by a rule-based logic outside of the MPC algorithm to reduce the computational burden of the MPC algorithm. See a flowchart of the rule-based logic in section 4.2. There are two driving modes considered: The first is when the two motors provide the propulsion needed by a 50:50 torque split and the second is when the rear motor provides the driving propulsion, and the front motor is called upon when the torque on the rear motor exceeds a certain threshold. In the same way, the front motor provides the braking torque, and the rear motor is called upon when the torque on the front motor exceeds a fixed threshold(Zheng, Tian & Zhang, 2020).

Finally, balancing the tradeoff between what one can call acceptable tracking performance and energy management. One often must decide what is an acceptable tracking offset which does not degrade the overall vehicle performance(Yang et al., 2021). In this project, an acceptable tracking is set as one which does not exceed $\pm 1\%$ of the speed profile.

1.5 Project Overview

The next set of chapters and sections covers the following: Chapter 2 covers the background information of the project. In this section, a case will be made for the use of optimization-based and/or rule-based techniques. Several other approaches will be discussed with their merits and demerits. In chapter 3, a detailed description of the vehicle model is given. Chapter 4 focuses on the nonlinear MPC implementation and a description of the rule-based logic used to further optimize the powertrain. Finally, chapter 5 outlines the results

compared to the baseline performance for both the MPC and the MPC+Rule-based Controller and chapter 6 analyses the results. Finally, chapter 7 discusses the conclusions drawn from this project and motivates future research directions.

2

CHAPTER TWO: BACKGROUND INFORMATION

Contents

2.1 Brief History of Energy Management in Electric Vehicles

The history of energy management in Battery Electric Vehicle (BEV) is intertwined with its predecessor, the Hybrid Electric Vehicle (HEV). Therefore, it is difficult to track the history of progress in energy management technologies without delving into the improvements made in HEV. For this reason, the term 'Electric vehicle' will imply either hybrid or pure battery electric vehicles.

According to Johnson et al as cited by Cavanini et al, 2022, the first attempt to improve energy efficiency in electric drivetrains was based on the classical rule-based approach. This method has the benefit of low computational burden but is heavily dependent on the drivetrain architecture and engineering intuition. Hence it was quite difficult to have an agnostic design

for improving the efficiency of Electric vehicle drivetrains(Cavanini et al., 2022). According to Musardo et al (2005) because of the growing need for more efficient and modular approach to solve the energy management problem in HEVs, the Equivalent Consumption Minimization Strategy (ECMS), became the standard approach for solving problems associated with energy management for many years(Musardo et al., 2005).

Nowadays, automative companies are beginning to adopt the model predictive control approach to solve the range anxiety problem in electric vehicles(Cavanini et al., 2022). The classical rule-based approach has been used in solving energy management problems, however it had a lot of limitations, among which is a lack of a fit-for-all design approach and suboptimal solution. This provided the needed justification and emphasized the need for the use of more advanced control techniques like model predictive control as a control strategy as it overcomes the limitations of the rule-based approach. The model predictive control approach holds the promise of resulting in an optimal solution at every time step throughout a prediction horizon and it results in a relatively modular solution compared to classical rule-based solutions(Louback et al., 2024).

2.2 Energy Management Strategies in Battery Electric Vehicles

Battery Electric Vehicles also called All Electric Vehicles like every other class of EVs are known for their use of a battery as source of power and for storage, electric motors for propulsion, an onboard charger, a pair transmission and axle which connects the electric motor and axle and, the transmission to the wheels respectively (*See figure 2*). The most prominent and perhaps relevant feature of this class of electric vehicles is the absence of an internal combustion engine which leads to zero atmospheric pollution emission(*Overview of Electric Vehicles in India*, 2020).

Due to the good dynamic characteristic of BEVs, they have been shown to provide far better performance in terms of energy efficiency by utilizing optimization-based techniques for energy management through torque control. However, their performance also largely depends on the optimization algorithms and their computation load (Karthika & Padmasuresh:, 2022).

As already highlighted above, an effort will be made in this writing to explore the two main approaches: rule-based and optimization-based approaches. There is also a third and fast-growing approach which is the reinforcement-learning based approach. However, this will not be discussed here. For more information on reinforcement learning-based approach, consult the article by Louback et al., (2024).

2.3 Energy Management Control Strategies

2.3.1 Rule-based Approach

There are two major types of rule-based EMS approaches: Deterministic and Fuzzy logic type. Rule based energy management approaches have been used for a long time to improve the energy performance of electric vehicles. These rules, which rely on heuristic techniques, human intelligence or mathematical models, require thorough understanding of the underlying system mechanisms. Since rule-based EMS approaches rely heavily on human intuition and engineering expertise, they often result in suboptimal solutions and are often too simplistic for practical applications. However, they have the advantage of not requiring foreknowledge of the drive cycle, they are simple to implement and hence computationally efficient(Wang, Zhou & Rizzoni, 2022).

An example of a practical deterministic rule-based approach derived from extensive powertrain efficiency studies is that the optimal split for independently driven axles (IDA) is 50:50 beyond a certain torque demand threshold. But below this threshold, the power train is more efficiently driven by one of the motors which serves as the primary traction element(Louback et al., 2024). To guarantee optimal energy performance, the foregoing statement is important even in the design optimization-based controllers for EV drivetrains. There is however no unified approach to rule-based EMS due to the variation in power train architecture, components and engineering expertise(Wang, Zhou & Rizzoni, 2022).

2.3.2 Optimization based Approach

There exist two major classes of optimization-based strategies: Global optimization and real time optimization-based approaches. They both rely on the use of cost function which is

optimized subject to some equality or inequality constraints (Karthika & Padmasuresh:, 2022). In global optimization, an optimal solution is computed offline based on knowledge of the demand dynamics for a known drive cycle. This is usually used as a baseline controller for most systems. In real time optimization, an optimal solution is computed online at every time step and implemented even when the drive cycle information is unknown(Huang et al., 2016).

Compared to the rule-based EMS approaches, optimization-based approaches enable the engineer to achieve optimal performance by solving a multi-objective quadratic or nonlinear problem subject to one or more constraints without the need for thorough understanding of the underlying engineering mechanisms at play in comparison to rule-based approaches(Louback et al., 2024).

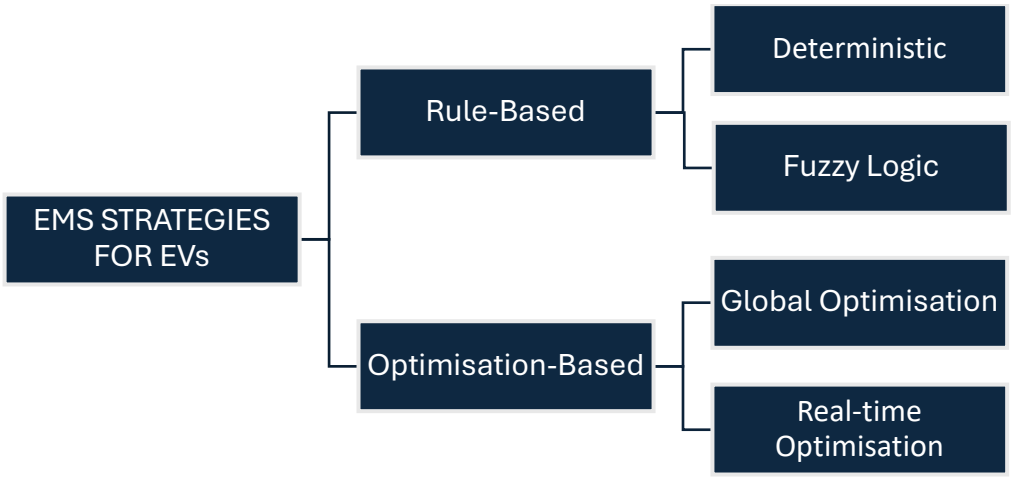

Figure 1: Electric Vehicle Energy Management strategies (Karthika & Padmasuresh:, 2022:p2)

Some examples of real-time optimization techniques include, Equivalent consumption and minimization strategy (ECMS), Particle swarm optimization (PSO), Model predictive control (MPC) etc (Karthika & Padmasuresh:, 2022). Since this project focuses more on MPC approaches, it will be investigated with greater depth.

2.4 Model Predictive Control

Model predictive control (MPC) has its origin in optimal control. It uses information about the system model, previous states or past measurements to decide on the optimal control action. It solves the regulation problem using model forecast and the estimation problem

using past measurements. An optimal trajectory within a given prediction horizon is computed online, part of the solution is implemented within a control horizon, and the process is repeated over the entire drive cycle in a moving horizon framework. To re-state one major benefit of the use of Model predictive control approach, which also has been outlined above, is in its ability to handle multiple constraints and objectives. However, this comes at the cost of a high computational burden. Since it is often important to achieve computational efficiency, it is always important to compare controller performance in terms of computational efficiency and resources required to achieve optimal (Rawlings et al, 2022: Schwenzer et al, 2021).

As more research is being done to optimize electric vehicle energy management systems, Model predictive controllers have been shown to offer the most promises for improvement of energy efficiency performance in all electric vehicles. Torque demand control is a recent approach for BEV drivetrain optimization (Karthika & Padmasuresh:, 2022) which this work seeks to explore in detail.

2.5 Model Predictive Control for Dual-Motor BEVs

Research into improving the efficiency of the DM BEV powertrain is a current hot topic in the automotive industry and in academia. It is quite a challenging problem to solve as several considerations, which include switching modes, optimal torque distribution and real time applicability seem to pose a multifaceted challenge. It is well known that the efficiency of the powertrain depends on the operating speed and torque values. It is often more efficient for the DM BEV to operate in a single driven mode at certain lower thresholds and switch to dual motor mode at medium or high thresholds. The challenge is designing an algorithm which integrates all these considerations to improve the overall energy performance of the drivetrain(Zheng, Tian & Zhang, 2020).

Zheng, Tian and Zhang, 2020 proposed:

'a three-layer energy management strategy composed of demanded torque calculation layer, mode decision layer and torque split layer to enhance the total operating efficiency of two motors'(p2).

In their work on the dual motor powertrain, they used particle swarm optimization to implement an optimal torque distribution. A rule-based algorithm which uses Genetic Algorithm (GA) to determine the optimal torque value for mode switch. This resulted in significant improvement in performance compared to conventional evenly distributed torque split strategy(Zheng, Tian & Zhang, 2020).

The torque demand approach has been shown largely to be suitable for use in improving the efficiency of battery electric vehicle drivetrains. This was also demonstrated by (He et al., 2021). They showed that energy savings can be made by designing a model predictive control law which optimized energy consumption. This resulted in about 1.67% in the city highway drive cycle compared to the baseline controller used (He et al., 2021).

The work done by (Yang et al., 2021) demonstrates the potential of nonlinear model predictive control in energy efficiency improvements. It utilizes a vehicle dynamic model of a BEV and a power loss model of an Interior Permanent Magnet (IPM) drive to solve an optimization problem which minimizes the power loss subject to input and output constraints. He further showed comparative performance of two torque distribution approaches implemented with PID controllers and compared the results to the performance (tracking and energy efficiency) of non-linear model predictive control. The two baseline PID based torque distribution approaches are the so call 'Greedy algorithm' based torque distribution and the 'fixed ratio' torque distribution.(Yang et al., 2021). The result showed that all three approaches achieved satisfactory tracking performance. Non-linear model predictive control however showed superior performance in energy efficiency. However, the aspect of computational burden and suitability for real time application were not discussed.

For an efficient real-time implementation of a model predictive control law in hybrid electric vehicles, Cavanini et al, 2022 developed a linear parameter varying MPC which was deployed in a processor-in-the-loop test. A relatively low fidelity linear parameter varying model of a

hybrid electric vehicle was used to approximate the nonlinear model of the plant. And an efficient real-time control law was implemented in a moving horizon to optimize the energy used(Cavanini et al., 2022). The method formulated a linear state space model with velocity as an external varying parameter to model the non-linear system. This method while suitable for hybrid electric vehicles control where an optimal energy distribution is developed in real time for the ICE and electric motor prime movers, may not be suitable for dual motors BEV powertrain as the dynamics of the two motors are identical and there is little to no effort in literature (based on this author's knowledge) on the use of linear parameter varying approaches for MPC controller design in dual motor BEV.

It has already been highlighted that one major challenge is in choosing a suitable model which adequately approximates the system to be controlled. This is important as the model must be able to meet the control objectives. While Cavanini et al, (2022) addressed the computation burden of the MPC problem formulation by using a linear parameter varying model of the system, his approach is highly situation dependent, and it may not be suitable for other problem cases or control objectives. (Yang et al., 2021) used a much-improved model in terms of fidelity, but at the expense of computational complexity. Hence it is clear that a trade-off must always be made between high fidelity model which usually results in computational complexity or a low fidelity approximation which may often oversimplify the model and make it less suitable for multi-objective optimization. Over-simplification often narrows the suitability of the model to only specific applications or control objectives(Cavanini et al, 2022: Yang et al,2021).

2.5.1 General Formulation of a Nonlinear MPC Problem

Given a nonlinear system model (Schwenzer et al., 2021):

$$x(k+1) = f\big(x(k), u(k)\big)$$

$$y(k) = g(x(k))$$

Where x is the system state, u is the input (manipulated variable) and y is the system output (manipulated output). $f(x,u)$ and $g(x)$ are the states and output functions respectively.

MPC minimizes a cost function given as:

$$J\big(x(k),u(k)\big) = \sum_{i=1}^{N_p} (J_{yt} + J_{uu})$$

Where $J_{yt}, and\, J_{uu}$ are components of the cost function $J(x,u)$ which achieves specific objectives. The objectives could be tracking the output (J_{yt}) or minimizing the control effort J_{uu}, subject to constraints below:

$$u_{lb} \leq u(k+j|k) \leq u_{ub}$$

$$x_{lb} \leq x(k+i|k) \leq x_{ub}$$

$$y_{lb} \leq y(k+i|k) \leq y_{ub}$$

$$\forall i \ \in \{0,\dots,N_p\}\, and\, j \ \in \{0,\dots,N_u\}$$

Where u_{lb}, u_{ub} are the lower and upper bounds of the control effort. x_{lb}, x_{ub} are the lower and upper bounds of the system states and y_{lb}, y_{ub} are the lower and upper bounds of the system outputs.

$x(k+i|k)$ is the predicted k+i state at k time step. A sequence of states is represented by $x(\cdot)$;

$x(k+i)\ \forall i \ \in \big(0,\dots,N_p\big) \rightarrow x(\cdot)$,

$u(k+i)\ \forall i \ \in (0,\dots,N_u) \rightarrow u(\cdot)$,

$y(k+i)\ \forall i \ \in \big(0,\dots,N_p\big) \rightarrow x(\cdot)$

2.6 Numerical Considerations for the Control of Stiff Systems

Stiff systems are those which incorporate several subsystems with widely different time constants. These systems show remarkable differences in the time varying speed of the subsystems which make up the whole. Because of the different time constants, these classes

of systems are prone to numerical instability issues when explicit discretization techniques are used in control applications. Stiffness is usually estimated by taking ratio of the largest (τ_{max}) to the smallest (τ_{min}) time constant exhibited by all the subsystems which make up the overall system model (Thomas, 1999).

$$Stiffness\ Coefficient, S = \frac{\tau_{max}}{\tau_{min}}$$

A system is classified as stiff if its stiffness coefficient exceeds 100 and not stiff if it is below 10(Thomas, 1999).

Other definitions of stiff systems exist in literature.

'Some literature defines stiff systems as systems which cannot be solved by explicit methods and their step sizes depend on stability requirements rather than accuracy. However, it is more broadly defined for nonlinear systems as a system whose Jacobian matrix has eigen values which vary widely in magnitude' (Illinois Institute of Technology, nd).

The system model under consideration in this project is composed of vehicle body, motors and battery subsystems. Their typical time constants are 5-10 seconds (rule of thumb), 0.02 seconds and 0.001 seconds (in battery voltage) respectively. Considering this widely varying dynamics, the dual motor battery electric vehicle is considered a stiff system, and careful attention must be paid to the discretization time step to overcome the instability which result from the use of explicit methods. To completely sidestep this challenge, a first order implicit Euler method is preferred to discretize the continuous time model state function. Fortunately, this is the default discretization method deployed by the solver used to solve the optimization problem(MathWorks, 2024a).

2.7 Gaps in the Literature

As seen in the work by Yang et al, 2021, Model predictive control has been used to design controller which distributes the torque for IPM motors with dynamics which can be modeled by mathematical equations. Where the power loss model was estimated under less intensive driving scenarios. However, motor dynamics are usually based on manufacturers data.

Hence this is just a suitable simplification. In this research however, the relatively more realistic data sheet motor model used, is based on the manufacturers data based on MathWorks 'Electric 2EM Vehicle' reference application. However, the detailed dynamics of the motors are not included in the prediction model.

Despite the recent more advanced work done to optimize dual motor drivetrain, much more still needs to be done in improving the computational burden of current dual motor battery electric vehicle. Several well-established techniques have been successfully implemented in other drivetrain architectures. But none has explored reducing the computational burden of relatively high-fidelity models in MPC applications. Even though the aspect of computational efficiency will be highlighted, this research does not claim to develop a computationally efficient algorithm for real-time implementation in DM-BEVs. This could become a suitable area to explore for further and more advanced work.

Throughout this research effort, Gain-scheduling and Linear parameter varying (LPV) approximations of nonlinear systems were explored. Their simple approximations of nonlinear models show lots of promises. However, they have a few challenges. LPV may not be suitable for some applications, for example, systems with fast dynamics may lead to instability issues in implementation. This could probably be salvaged by the recent velocity based LPV modeling. The VBLPV is superior in that it does not require linearization; it represents the nonlinear dynamics of a system validly around all operating points rather than just at equilibrium points as in the case in LPV or quasi LPV structures. One challenge though is that the quasi LPV structure of VBLPV systems lead to models which might be difficult to control (Grimble & Majecki, 2020). Gain scheduling, however, takes linear approximations of the controller at several operating equilibrium points which may also result in instability issue for systems with fast changing dynamics. However, it avoids the LPV or quasi LPV structure which are relatively difficult to control(Grimble & Majecki, 2020). Even though this modeling approach was considered at the beginning, it was not used due to limitations in the author's knowledge. This research project does not apply LPV techniques in its approach. However, the author thought it necessary to highlight this important unexplored area which might aid real time implementation.

3

CHAPTER THREE: SYSTEM MODEL

Contents

3.1 Electric Vehicle Architecture

In this section a description of electric vehicle architecture and parameterization is given based on the MathWorks reference application: 'Electric Vehicle 2EM'(MathWorks, 2022). The vehicle architecture is the dual motor coupling powertrain with parallel architecture made of two electric motors which provides torque to the front and rear wheels. The Electric Vehicle power train is illustrated in figure 2 below showing the Energy management system. This energy management system determines how the torques (T_{em1} and T_{em2}) from the motors are distributed. The reference torque demanded by the driver to control the speed of the vehicle is given by T_{ref}(Cavanini et al., 2022).

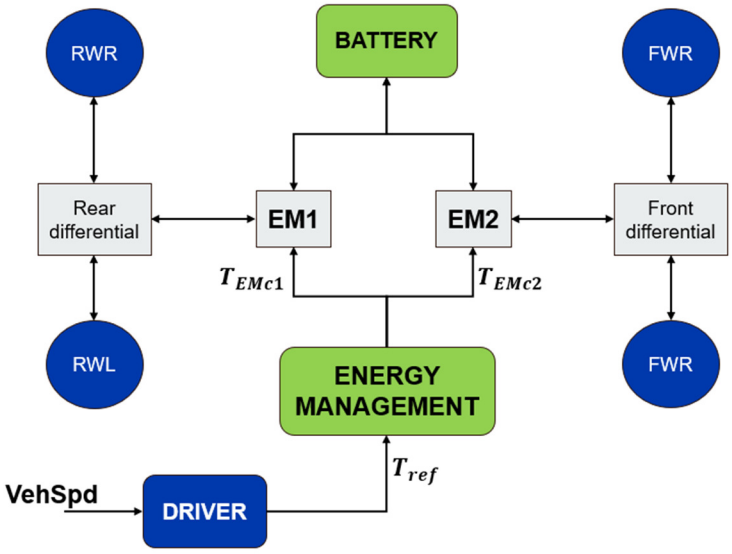

Figure 2:DM-BEV-IDA Architecture (Cavanini et al., 2022:p2)

The Energy management system allocates the command torque to the electric motors (EM1 and EM2) which are the inputs which drive the rear (RWR and RWL) and front (FWR and FWL) wheels respectively. The vehicle speed (VehSpd) determines the reference torque. There is a bidirectional flow of energy between the battery and the motors. The motor consumes energy during forward driving and regenerates energy during braking. The motors are connected to the wheels through the rear and front differentials with a final drive ratio of 3.32. The transmission and axle efficiency are given as 0.98(MathWorks, 2022).

3.2 Vehicle Longitudinal Dynamics

The vehicle dynamics is a one degree of freedom (1DOF) model, suitable for energy efficiency studies. It consists of a rigid body block mass in either reverse or forward motion. Lateral movement of the vehicle is not considered as it does not impact the energy performance of the vehicle significantly. Also, vertical movement of the vehicle is considered negligible(MathWorks, 2023b).

The longitudinal motion of the vehicle is given by the equation below:

$$m\dot{v} = F_{trac} - F_{roll} - F_{drag}$$

$$F_{trac} = F_{pwt} - F_{brake}$$

$$F_{roll} = \frac{C_r mg}{2}$$

$$F_{drag} = \frac{1}{2RT}.A_f.C_d.P_{abs}.v^2$$

$F_{pwt} = \frac{T_{wh,i}}{r} = \frac{T_{em,ifdr}}{r}$ where $T_{wh,i}$ is the torque at the ith axle (front or rear).

Where F_{trac} is the traction force provided by the two electric motors after considering the resistance from the brakes F_{brake} , F_{roll} is the rolling resistance and F_{drag} is the resistance due to the aerodynamics properties of the vehicle's interaction with the environment (Rajamani, 2012). $T_{wh,i}$ is the ith wheel torque and $T_{em,i}$ is the ith motor torque.

The parameters of the longitudinal vehicle model are taken from the "MathWorks: Electric Vehicle 2EM" model from the Virtual Vehicle Composer App in the Powertrain block set. The parameter values and description are captured in the table below (MathWorks, 2022).

Table 1:Vehicle dynamics Parameters (MathWorks, 2022)

Symbol	Parameter	Value	Unit
M	Mass of vehicle	1623	kg
R	Atmospheric specific gas constant	287.5	
T	Environmental abs temperature	293.15	
$\boldsymbol{A_f}$	Vehicle frontal area	2.27	m^2
$\boldsymbol{C_d}$	Air drag coefficient	0.336	
$\boldsymbol{P_{abs}}$	Absolute pressure	101325	Nm
G	Acceleration due to gravity	9.81	m/s
$\boldsymbol{C_r}$	Rolling resistance	0.01	
$\boldsymbol{\gamma}$	Road grade	0	Deg'

3.3 Traction Forces

The forces propelling the vehicle through the wheels are given by the equations below

$$F_{trac} = F_{tracEM1} + F_{tracEM2}$$

$$F_{trac} = (\sum_{i=1}^{4} T_{Whi} - T_{brakei})/r$$

Wheel speed $\omega_{wh} = \frac{v_{eh}}{r}$

Where $F_{tracEM1}$ and $F_{tracEM2}$ are the traction forces provided by the front and rear motors respectively. T_{Wh}, T_{brake} and r are the traction torque on the wheels, braking torque on the wheels and radius of the wheel respectively.

The total traction force is the sum of the forces supplied to the front and rear set of wheels. Note that Braking torque is neglected in the prediction model in chapter 4 as it is negligible for most duration of the drive cycle.

3.4 Electric Motor Dynamics

The electric machine is modelled by a mapped motor operating in torque control mode. This mapped motor takes the battery voltage and electric motor speed as inputs, while the output is the battery current and mechanical torque from the electric motor (MathWorks, 2023b). This motor speed is computed from the vehicle speed as a suitable approximation neglecting the effect of slip on the wheels.

The speed at the front and rear wheels are equal in torque control mode(Louback et al., 2024).

The motor speed in rpm is computed considering the final drive ratio of the rear and front differential such that:

$$\omega_{EM1} = \omega_{EM2} = \frac{v_{eh}}{r}.f_{dr}$$

Table 2: Powertrain Parameters (MathWorks, 2022)

Symbol	Parameter	Value	Unit
f_{dr}	Final drive ratio	3.32	
r	Loaded radius of the wheel	0.327	M
τ_e	Motor / power electronics response	0.02	

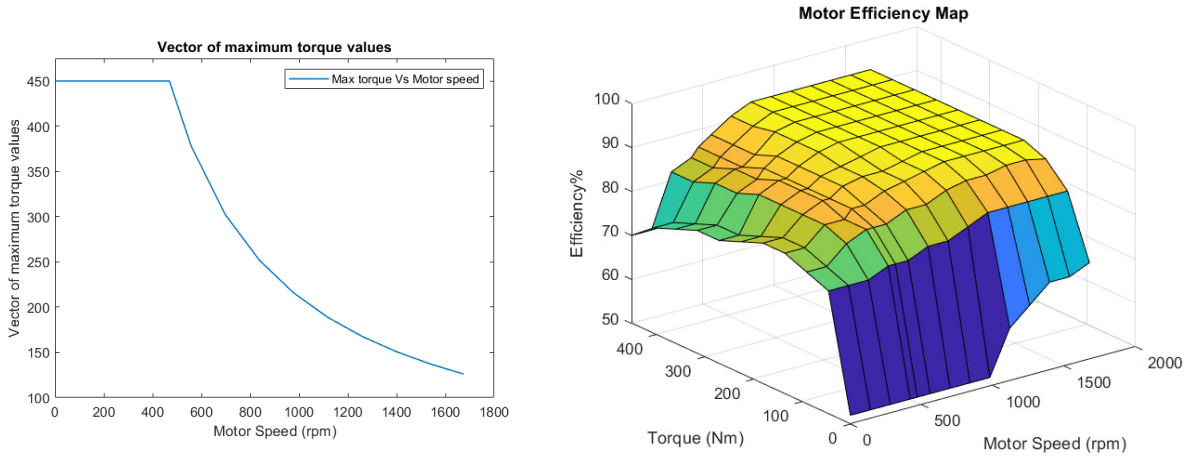

(a) Torque vs Speed curve (b) Efficiency map

Figure 3: Electric Machine Characteristics (MathWorks, 2022)

3.5 Differential

This consists of a 50-50 split of the torque supplied by the motor, between the left and right wheels. With a final drive ratio of 3.32 and axle efficiency of 0.98. (MathWorks, 2023b). The efficiency of the differential is neglected in the prediction model in chapter 4.

3.6 Transmission

The efficiency of the transmission is 0.98, taking the input torque as the torque output from the motor and output as the torque input to the vehicle axles.(MathWorks, 2023b). The efficiency of the transmission is neglected in the prediction model as will be seen in chapter 4.

3.7 Battery

The battery model is a datasheet battery block parameterized by the manufacturers data. It uses a look up table to determine the battery output voltage by implementing the open circuit voltage and internal resistance as function of temperature and battery state of charge(MathWorks, 2023b).

As captured also in the MathWorks Powertrain reference guide(MathWorks, 2023b):

$$E_m = f(SOC)$$

$$R_{int} = f(T, SOC)$$

$$V_T = E_m - I_{batt} R_{int}$$

$$I_{batt} = \frac{I_{in}}{N_p}$$

$$V_{out} = V_T N_s$$

Where E_m is the open circuit voltage per battery, R_{int} is the internal resistance, V_T is the output voltage per battery and V_{batt} is the combined output voltage of all the battery modules. I_{batt} is the current flowing out of a single battery and I_{in} is the total current flowing from the battery network(MathWorks, 2023b).

For simplicity, this output voltage V_{batt} is taken to be constant in the prediction model throughout the drive cycle. The constant value is derived by taking a rough median value from observation of the voltage variation during a typical baseline-controlled drive cycle.

As seen in the MathWorks Powertrain reference guide (2023b):

$$SOC = SOC_o - \frac{1}{Q_c} \int_0^t I_{batt}\ dt$$

Where $Q_c = Q_{batt} * N_p$

Where $SOC_o = Q_c * 0.6$. where the initial battery charge is 60%.

Where SOC is the battery state of charge, SOC_o is the initial battery charge, V_{batt} is the battery output voltage assumed to be constant, and Q_c is the battery capacity.

Table 3: Battery Parameters (Mathworks, 2022)

Symbol	Parameter	Value	Unit
$\boldsymbol{SOC_o}$	Initial battery state of charge	177.83	Ah
$\boldsymbol{Q_c}$	Maximum capacity of battery	296.382	Ah
$\boldsymbol{V_{batt}}$	Average battery output voltage	355	volts
$\boldsymbol{N_s}$	Number of batteries in series	96	
$\boldsymbol{N_p}$	Number of batteries in parallel	94	
$\boldsymbol{Q_{batt}}$	Maximum charge per battery	3.153	Ah

3.8 Nonlinear EV Powertrain Dynamics

The overall model dynamics is summarized and given below:

$$\dot{v}_{eh} = \frac{1}{m}(F_{trac} - F_{drag} - F_{roll})$$

$$S\dot{O}C = -\frac{1}{Q_c V_{batt}}\left(\frac{T_{EM1}\omega_{EM1}}{\eta_{EM1}} + \frac{T_{EM2}\omega_{EM2}}{\eta_{EM2}}\right)$$

Where $I_{bat} = \frac{-1}{V_{batt}}\left(\frac{T_{em1}\omega_{em1}}{\eta_{EM1}} + \frac{T_{em2}\omega_{em2}}{\eta_{EM2}}\right)$

Since $T_{EM1c}, = T_{EM1}$ and $T_{EM2c}, = T_{EM2}$ at equilibrium points. We can further simplify the 4-state model to 2 to reduce the computational burden. This results in a reduced order model state function. Note that efficiency for each motor is ignored in the non-linear prediction model below.

$$\dot{v}_{eh} = \frac{1}{m_v}\left((T_{em1} + T_{em2})\frac{f_{dr}}{r} - \frac{1}{2RT}A_f C_d P_{abs} v_{eh}^2 - \frac{1}{2}C_r m_v g\right)$$

$$S\dot{O}C = -\frac{1}{Q_c V_{batt}}\left((T_{em1} + T_{em2})\frac{v_{eh} f_{dr}}{r}\right)$$

4

CHAPTER FOUR: CONTROLLER DESIGN

Contents

As with linear MPC, nonlinear MPC also solves an optimization problem which computes the control effort at every time step over a prediction horizon. It also uses a prediction model in a usually constrained environment. However, a few major differences are notable compared to the traditional linear MPC(MathWorks, 2024c):

The key difference with linear MPC as highlighted in the *MathWorks Model Predictive Control toolbox*:

> "The prediction model can be nonlinear and include time-varying parameters, the equality and inequality constraints can be nonlinear. The scalar cost function to be minimized can be a nonquadratic (linear or nonlinear) function of the decision variables"(MathWorks, 2024c)

Considering the non-linear model described in Section 3.8, the nonlinear model predictive controller will be designed using *MathWork's Model Predictive Control toolbox.*

4.1 MPC Controller Design

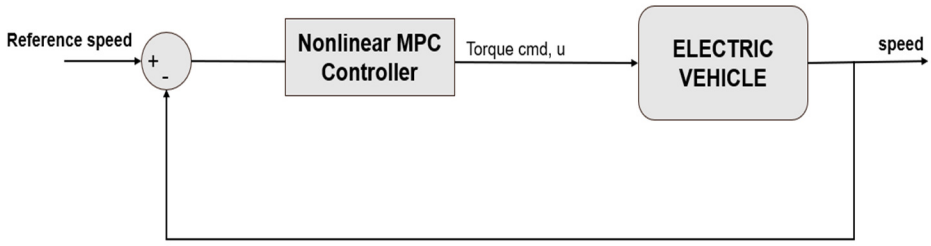

Figure 4: Closed loop with MPC controller

The controller is designed, which takes as input the error between the reference speed and the vehicle speed and computes an optimal torque which drives the vehicle to follow the speed profile while minimizing the control effort. The states considered are the vehicle speed and battery state of charge.

4.1.1 Prediction model

The prediction model consists of the state and output function. The state function derived from the model equations shown in section 3.8 shows how the system states evolve in time. The output function computes the output of the system using the state and input variables.

State Function and Jacobian

$$\dot{v}_{eh} = \frac{1}{m_v}((T_{em1} + T_{em2})\frac{f_{dr}}{r} - \frac{1}{2RT}A_f C_d P_{abs} v_{eh}^2 - \frac{1}{2}C_r m_v g)$$

$$S\dot{O}C = -\frac{1}{Q_c V_{batt}}((T_{em1} + T_{em2})\frac{v_{eh} f_{dr}}{r})$$

Where v_{eh} and SOC represents the speed and battery state of charge respectively. They also represent the states of the system. T_{em1} and T_{em2} represents the motor torques and inputs to the model.

The Jacobian is computed by taking the partial derivative of the state function with respect to the states (A_{jac}) and the partial derivative of the state function with respect to the

manipulated variables (B_{jac}). The Jacobian is an extra requirement to improve the computational efficiency of the solver(MathWorks, 2024c).

$$A_{jac} = \begin{pmatrix} -\frac{A_f\, C_d\, P_{\text{abs}}\, v_{eh}}{R_{\text{abs}}\, T_{\text{abs}}\, m_v} & 0 \\ -\frac{\frac{T_{em1}\, f_{\text{dr}}}{r} + \frac{T_{em2}\, f_{\text{dr}}}{r}}{Q_c\, V_{\text{bat}}} & 0 \end{pmatrix}$$

$$B_{jac} = \begin{pmatrix} \frac{f_{\text{dr}}}{m_v\, r} & \frac{f_{\text{dr}}}{m_v\, r} \\ -\frac{f_{\text{dr}}\, v_{eh}}{Q_c\, V_{\text{bat}}\, r} & -\frac{f_{\text{dr}}\, v_{eh}}{Q_c\, V_{\text{bat}}\, r} \end{pmatrix}$$

Where A_{jac} is a 2X2 matrix and B_{jac} is a 2X2 matrix both computed as described above.

Output Function and Jacobian

The output of the system is velocity.

$$y = v_{eh}$$

The Jacobian is computed by taking the partial derivative of the output function with respect to the states (C_{jac}) and the partial derivative of the output function with respect to the manipulated variables (D_{jac}).

$$C_{jac} = \begin{pmatrix} 1 & 0 \end{pmatrix}$$

$$D_{jac} = \begin{pmatrix} 0 & 0 \end{pmatrix}'$$

Where C_{jac} is 1X2 matrix and D_{jac} is 2X1 matrix.

Model Discretization

For models which are stiff: that have varying time constant and high nonlinearities, implicit discretization techniques are suitable because they are less prone to inaccuracy and instability(Thomas, 1999). The model equations are discretized using the implicit Euler discretization. The solver used in solving the constrained optimization problem uses by

default the implicit Euler which will be adopted for its optimal performance in relatively stiff systems(MathWorks, 2024a).

The discretization form using implicit Euler is shown below:

$$v_{eh,k+1} = v_{eh,k} + \tau\left(\frac{\frac{1}{m_v}\left(T_{em1,k+1} + T_{em2,k+1}\right)f_{dr}}{r} - \frac{1}{2RT}A_f C_d P_{abs} v_{eh,k+1}^2 - \frac{1}{2}C_r m_v g\right)$$

$$SOC_{k+1} = SOC_k - \tau\left(\frac{\frac{1}{Q_c V_{bat}}\left(T_{em1,k+1} + T_{em2,k+1}\right)v_{eh,k+1}f_{dr}}{r}\right)$$

Where τ is the discretization timestep size and k represents the time step within a prediction horizon p.

4.1.2 Constraint

The main constraints are input constraints.

Input Constraints: This includes constraints on the torque command to powertrain transmission

$u_{i,min} \leq u_i(k) \leq u_{i,max}\ \forall k = 0,1,2 \ldots p$

Where $u_{1,min} = -450\ Nm$ and $u_{1,max} = 450\ Nm$ and $u_{2,min} = -450\ Nm$ and $u_{2,max} = 450\ Nm$.

Where $u_1 = T_{em1}$ and $u_2 = T_{em2}$

Output Constraints: No output constraints were included in the problem formulation since one of the main objectives is to track the reference speed with the vehicle speed as the output.

Normal Load (F_z) Constraint: This constraint is described below

$$F_{z,min} \leq F_{zF} \leq F_{z,max}$$

$$F_{z,min} \leq F_{zR} \leq F_{z,max}$$

Where $F_{z,min} = 100\ N$ and $F_{z,max} = 6570\ N$

This constraint can be guaranteed analytically from the equation and computation shown below. It is also verified in simulation. There is no need to include this constraint in the optimization problem.

Assuming the main contributor to the normal load is due to the road angle as the vehicle is assumed to be vertical equilibrium and there are no other resultant forces or moment acting in the vertical axis. From the problem formulation, the road angle is given to be zero throughout the drive cycle.

Given that the rolling resistance on the wheels are given by(Rajamani, 2012):

$$F_{roll} = C_r(F_{zF} + F_{zR})cos\gamma$$

Where C_r is the rolling resistance coefficient, F_{zF}, F_{zR} are the normal load on the front and rear wheels respectively and γ is the road angle.

The equations below are given by He et al., (2021)

$$F_{zF} = \frac{m}{2(a+b)}(bg - h\dot{v})$$

$$F_{zR} = \frac{m}{2(a+b)}(ag + h\dot{v})$$

Substituted in the preceding equation

$$F_{roll} = \frac{1}{2}C_r mg$$

Implying that $F_{zF} + F_{zR} = \frac{1}{2}mg$. Since m = 1623kg and g = 9.81m/s.

$$F_z = F_{zF} + F_{zR} = 7960.8\ N$$

Where m is the mass of the vehicle, a and b are the distances of the front and rear axles from the projection point on the common axle of the vehicle's center of gravity and h is the height of the vehicle's center of gravity above the axle plane.

Hence the normal load is guaranteed to be satisfied throughout the drive cycle given the conditions described thus far. This assertion will be shown in simulation in the results sections in chapter 5.

Slip ratio Constraint ($\boldsymbol{\sigma}$)**:** This is described as follows:

$$\sigma = \frac{r\omega_{wh} - |v_{eh}|}{v_{eh}} \leq 0.6$$

This constraint cannot be parameterized in the problem formulation because wheel speed is not part of the system variables. Hence, this constraint is implicit to the model equations. In fact, the prediction model assumes that wheel speed is computed from known values of the vehicle velocity.

$$\omega_{wh} = \frac{v_{eh}}{r}$$

Hence this guarantees that the constraint will not be violated. It is also verified from simulation.

4.1.2 Cost function

This is specified as a scalar which penalizes deviation from the output reference values (tracking) and minimizes the control effort. Below is the discretized cost function:

$$J(x(k), u(k)) = \frac{1}{2}\sum_{1}^{p+1}\left(x(k) - x_{ref}(k)\right)' Q\left(x(k) - x_{ref}(k)\right) + u(k)'Ru(k)$$

Where x_{ref} is the reference trajectory of the vehicle which contains the drive cycle information, $Q\ and\ R$ are weighting matrices for penalizing deviation from the reference signal and control effort minimization respectively. $x\ and\ u$ are the state and input vectors respectively.

4.1.3 Non-linear MPC Solver

An efficient solver is often needed to solve an optimization problem especially one of this size and importance. Since the dynamics of a motor is quite fast, its computation must be fast enough to be able to look between 2 to 5 seconds into the future and operate with a time step

of between 10 -100milliseconds. For this task, the C/GRMES solver was used for its computational efficiency and its ability to solve optimization problems with stiff properties. This property provides a good tradeoff between very strong stability and accuracy. It uses by default the implicit Euler discretization (a first order discretization). However, it is not as accurate compared to second order discretization techniques like trapezoidal discretization (second order discretization)(MathWorks, 2024a). However, the default implicit Euler discretization is suitable for the current application.

Table 4: C/GMRES Configuration Settings (MathWorks, (2024c))

Parameter	Value
Stabilization Parameter	20
Maximum iterations	50
Restart	5
Barrier Parameter	0.1
Termination Tolerance	1e-11

4.2 MPC+Rule-based Controller Design

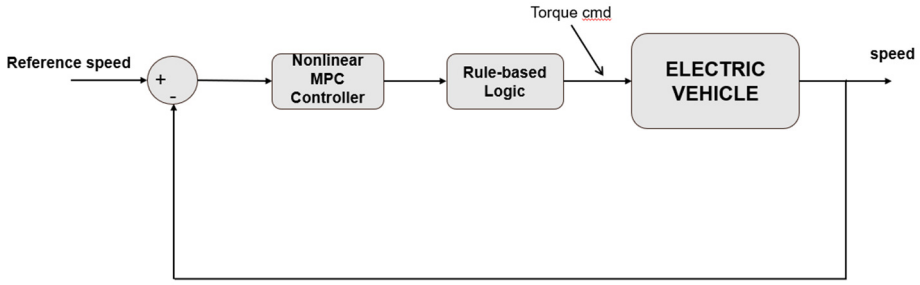

Figure 5: Closed loop with MPC+RB controller

This controller performs an extra processing of the optimal torque output of the MPC controller as shown in figure 4. The states considered here are still the vehicle speed and battery state of charge. All the other configurations are the same as that of the MPC controller designed in section 4.1 above. The rule-based logic is described below.

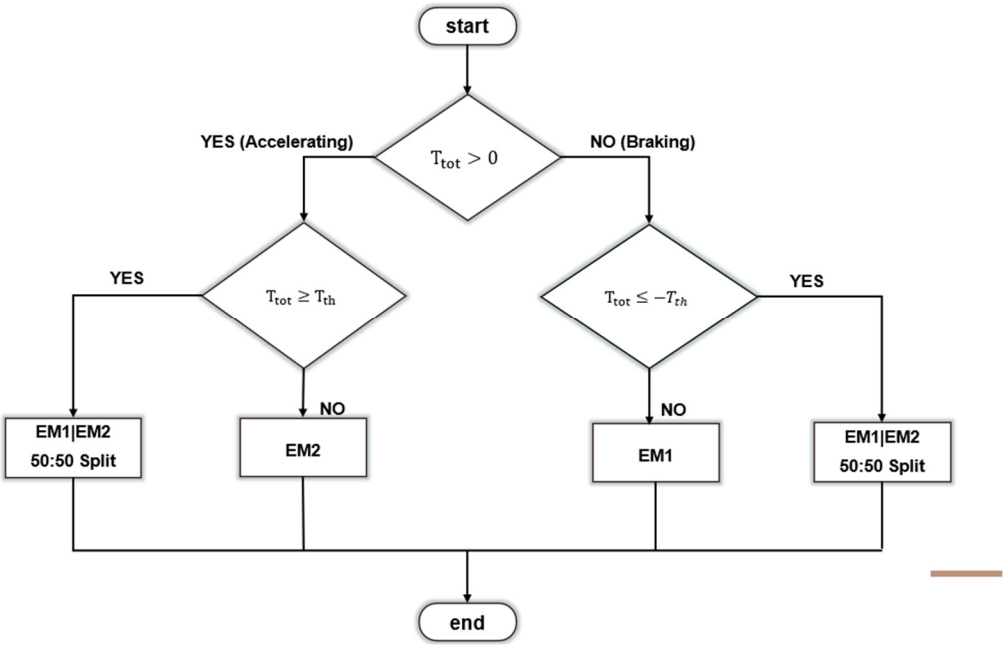

Figure 6: 'Rule-based Logic'(Zheng, Tian & Zhang, 2020)

The rule-based logic is a modification of that employed by Zheng, Tian and Zhang (2020) for optimizing the efficiency of a dual motor battery electric vehicle.

From figure 6 above, note that: T_{tot} is the total optimal torque as computed by the MPC controller while T_{th} is the threshold torque beyond which an optimal 50:50 split is performed. EM1, EM2 represents the front and rear electric motors respectively(Zheng, Tian & Zhang, 2020).

4.3 Stability

Considering the quadratic cost function as suitable Lyapunov function. The Lyapunov stability criteria guarantees that the system described above is stable if the Lyapunov function has positive definite weighting matrices Q and R, and its derivative is negative definite- Since the state always approaches the reference state at each time step, the error between the reference and state is guaranteed to decrease across the prediction horizon. Hence one can claim asymptotic stability. This is enough to guarantee stability of the closed loop(Angeli, 2012).

5

CHAPTER FIVE: RESULTS

Contents

5.1 Controller Simulation Description

In this section, the results for the performance of the baseline, MPC and MPC+RB controllers are shown for two drive cycles: WLTP Class3 and the HWFET drive cycles. And as a validation

step, the controllers are tested in the FTP75 and US06 drive cycles. Their performance was assessed and compared for tracking, energy efficiency, range and constraints violation.

The baseline controller is first described, and its performance on the four drive cycles mentioned above is shown to lay the foundation for future comparison with the nonlinear MPC and MPC+RB controllers.

5.2 Baseline Controller Description

The baseline controller implements a logic-based acceleration pedal to torque request, regenerative braking for maximum energy recovery and power management using the Hamiltonian computation and minimization which distributes the torque in the wheels(MathWorks, 2023a:p3-27).

5.3 Baseline Controller Performance

5.3.1 WLTP Class 3 Drive Cycle

The tracking performance compared to the drive cycle data and total energy consumption in percentage battery state of charge of the baseline controller is shown in the table below:

Baseline controller tracking offset and energy consumption for WLTP Class 3 Drive Cycle

Tracking/Range offset (%)	Energy consumption (%BSOC)
-0.1204	3.9999

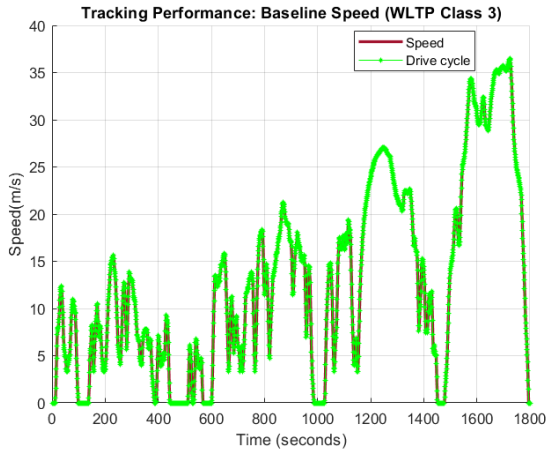

(a) Output tracking

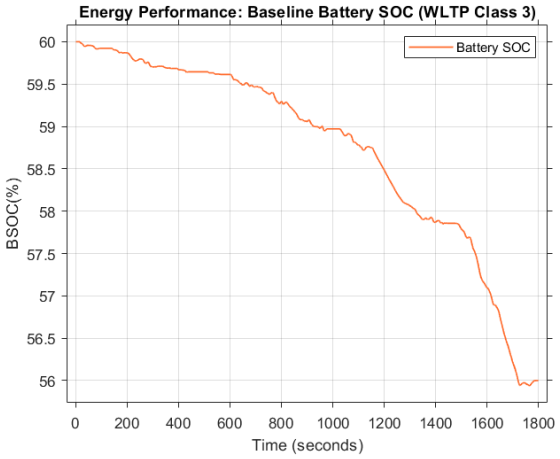

(b) Battery state of charge

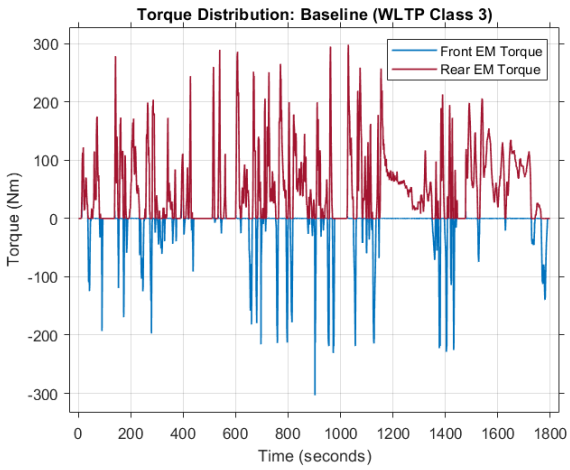

(c) Torque distribution

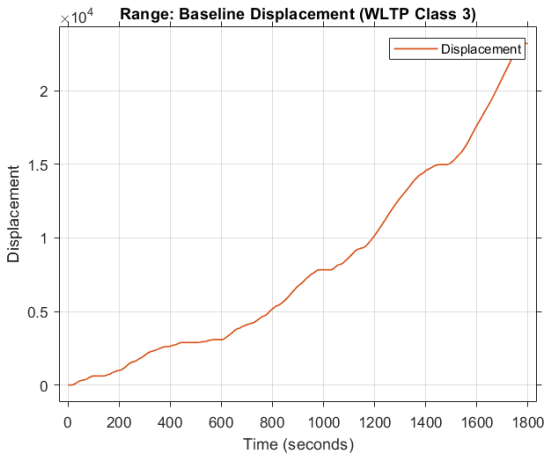

(d) Range of travel

Figure 7: Baseline Controller performance on WLTP Class 3 drive cycle (a-d)

5.3.2 HWFET Drive Cycle

The tracking performance compared to the drive cycle data and total energy consumption in percentage battery state of charge of the baseline controller is shown in the table below:

Baseline controller tracking offset and energy consumption for HWFET Drive Cycle

Tracking/Range offset (%)	Energy consumption (%BSOC)
+0.0094	2.5855

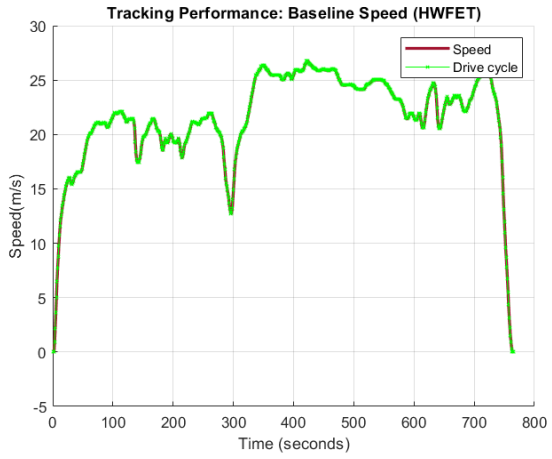

(a) Output tracking

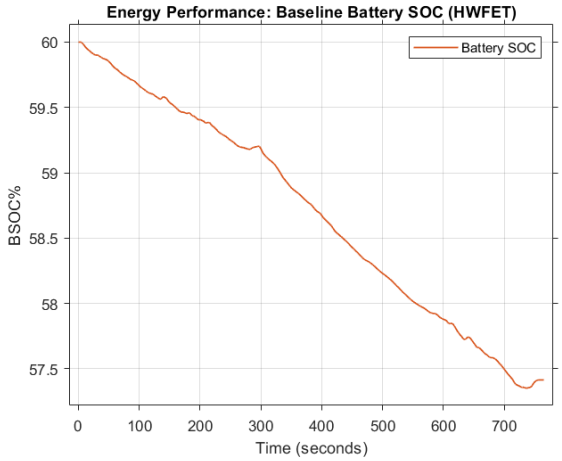

(b) Battery state of charge

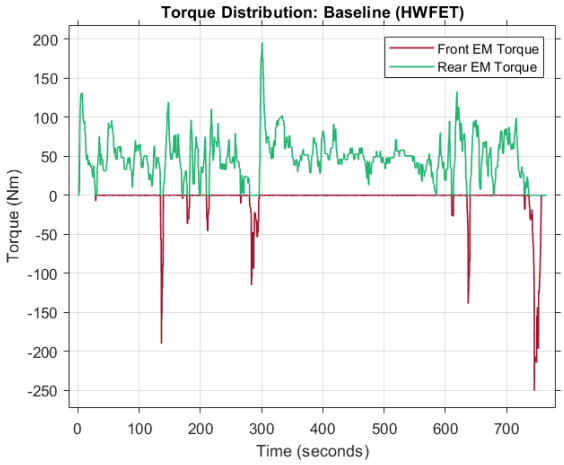

(c) Torque distribution

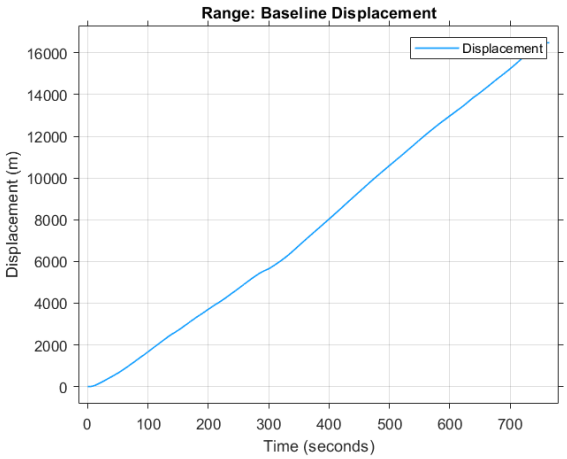

(d) Range of travel

Figure 8: Baseline controller performance on HWFET Drive Cycle (a-d)

5.3.3 FTP75 Drive Cycle

The tracking performance compared to the drive cycle data and total energy consumption in percentage battery state of charge of the baseline controller is shown in the table below:

Baseline controller tracking offset and energy consumption for FTP75 Drive Cycle

Tracking/Range offset (%)	Energy consumption (%BSOC)
-0.1570	2.5010

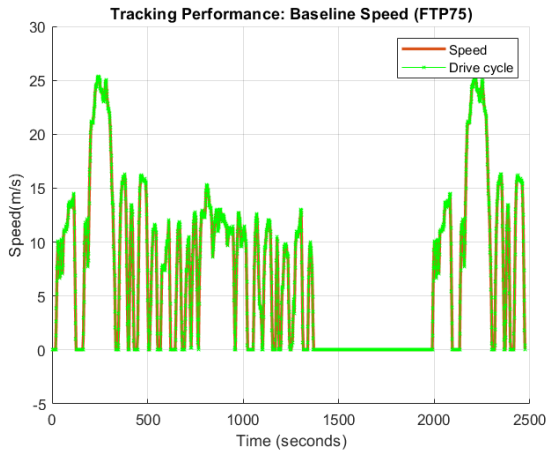

(a) Output tracking

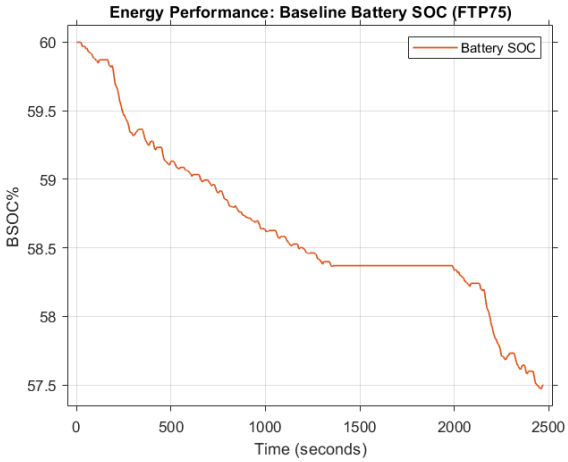

(b) Battery state of charge

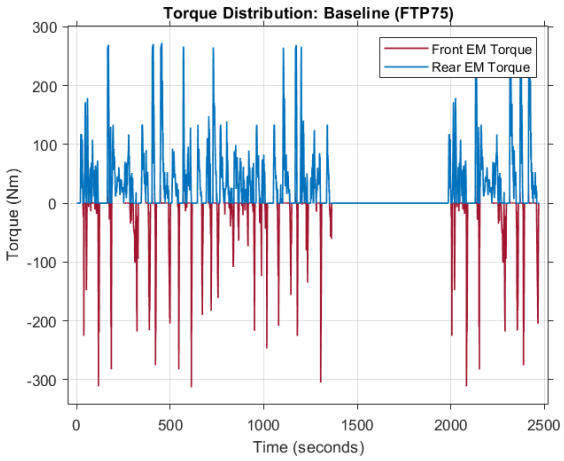

(c) Torque distribution

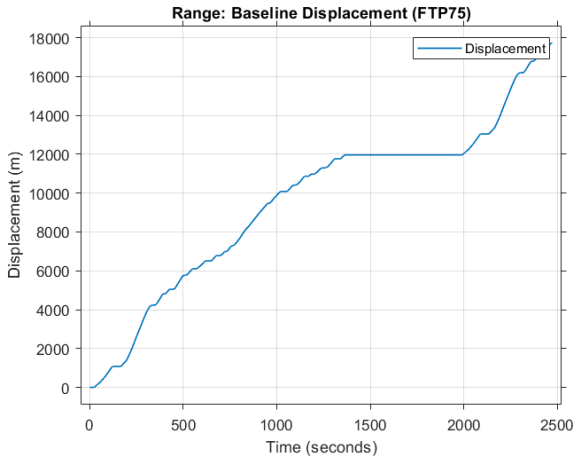

(d) Range of travel

Figure 9: Baseline controller performance on FTP75 Drive Cycle (a-d)

5.3.4 US06 Drive Cycle

The tracking performance compared to the drive cycle data and total energy consumption in percentage battery state of charge of the baseline controller is shown in the table below:

Baseline controller tracking offset and energy consumption for US06 Drive Cycle

Tracking/Range offset (%)	Energy consumption (%BSOC)
+0.0093	2.8915

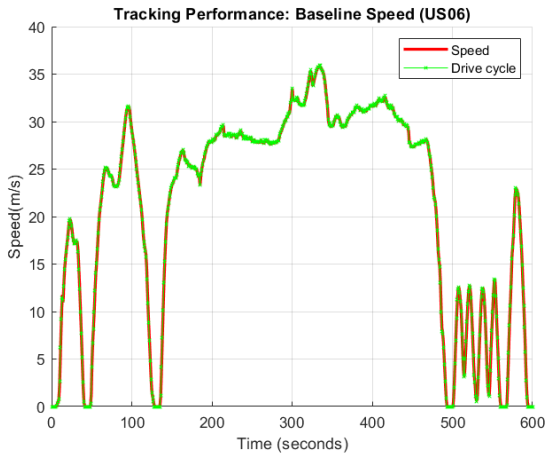

(a) Output tracking

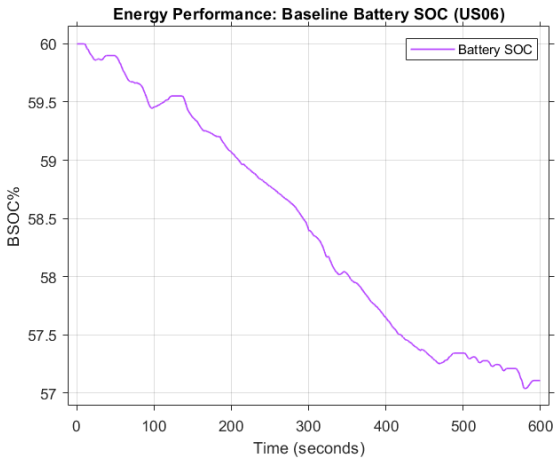

(b) Battery state of charge

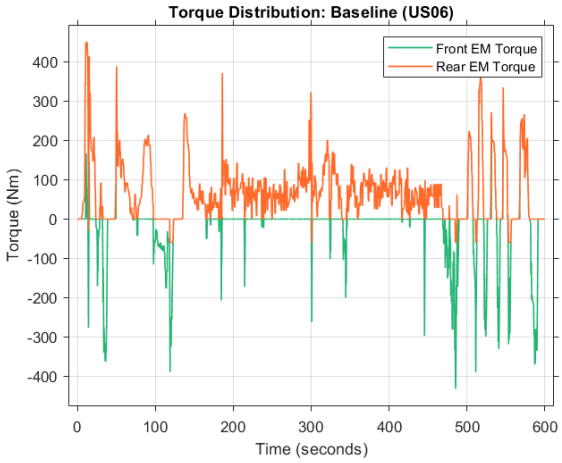

(c) Torque distribution

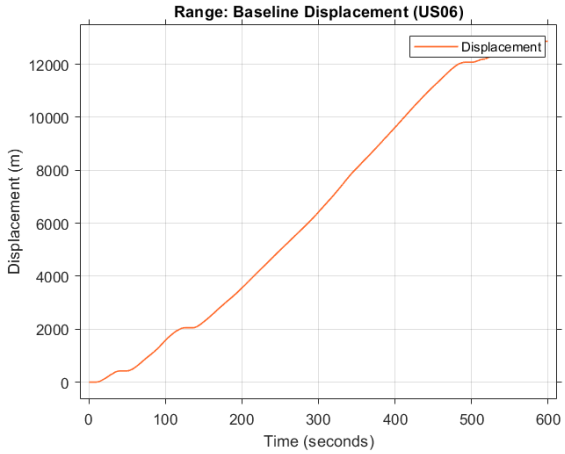

(d) Range of travel

Figure 10: Baseline controller performance on US06 Drive Cycle (a-d)

5.4 MPC Controller Description

The MPC controller is a nonlinear model predictive controller with equal weights on the control effort. Below is a table containing the controller parameters. The details of the prediction model, cost function and constraints are as described in chapter 4.

Table 5: MPC Controller Parameters

Symbol	Parameter	Value	Unit
$\boldsymbol{p}$	Prediction horizon	40	
$\boldsymbol{\tau}$	Time step	0.05	
$\boldsymbol{Q}$	Weight on output tracking	1000	
$\boldsymbol{R}$	Weight on control effort	**[0.1, 0.1]**	
$\boldsymbol{P}$	Prediction time	2	Secs

5.5 MPC Controller Performance

In this section, the results in terms of output tracking, amount of energy used, range covered, and constraints violation of the MPC controller will be shown for the WLTP Class 3, HWFET,

FTP75 and US06 drive cycles. Unlike the baseline controller, the MPC controller performs a 50-50 split in the torque between the two motors.

5.5.1 WLTP Class 3 Drive Cycle

The tracking performance compared to the baseline controller results and total energy consumption in percentage battery state of charge of the MPC controller is shown in table below. Figure 11 (e) and (f) also shows that the constraint on the slip ratio and normal load on each wheel were not violated.

MPC controller tracking offset compared to baseline and total energy consumption for WLTP Class 3 Drive Cycle

Tracking/Range offset (%)	Energy consumption (%BSOC)
-0.5291	3.9341

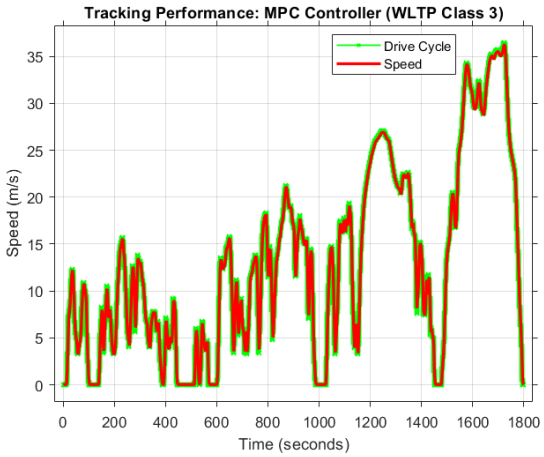

(a) Output tracking

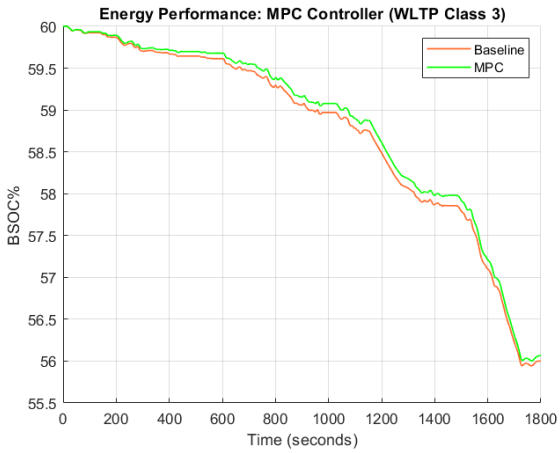

(b) Battery state of charge

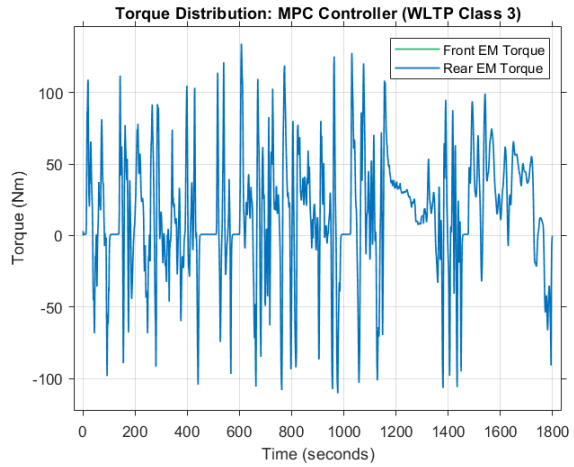

(c) Torque distribution

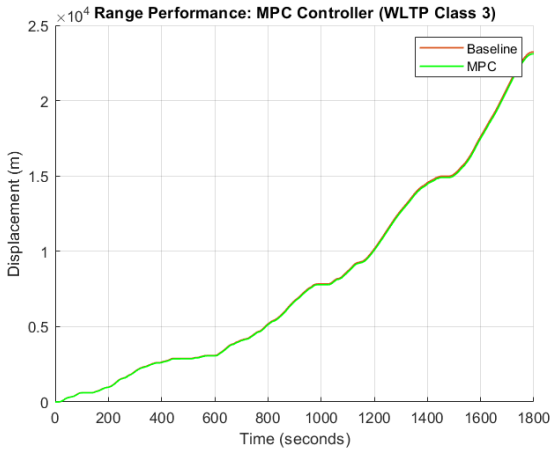

(d) Range of travel

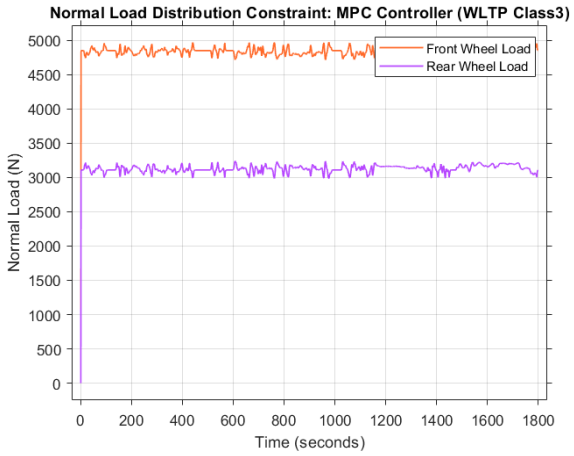

(e) Wheel Normal load

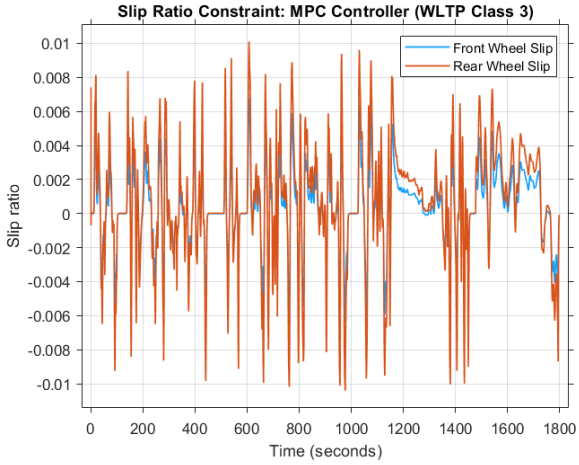

(f) Wheel slip ratio

Figure 11: MPC controller performance on WLTP Class 3 Drive Cycle (a-f)

5.5.2 HWFET Drive Cycle

The tracking performance compared to the baseline controller results and total energy consumption in percentage battery state of charge of the MPC controller is shown in table below. Figure 12 (e) and (f) also shows that the constraint on the slip ratio and normal load on each wheel were not violated.

MPC controller tracking offset compared to baseline and total energy consumption for HWFET Drive Cycle

Tracking/Range offset (%)	Energy consumption (%BSOC)
-0.4464	2.6089

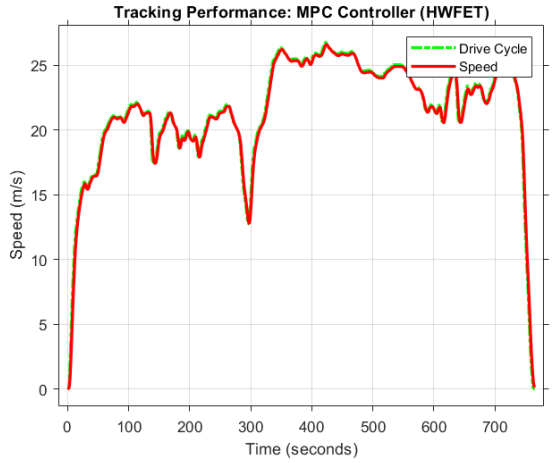

(a) Output tracking

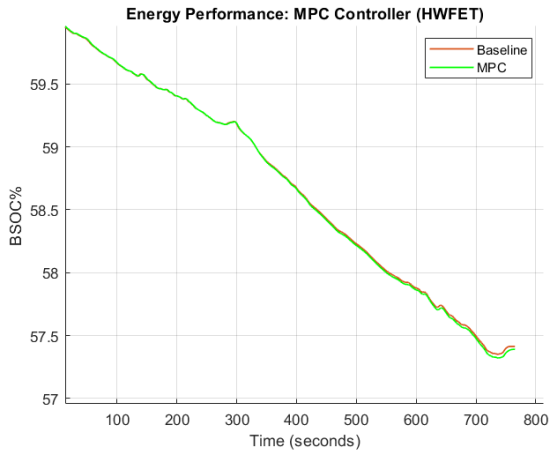

(b) Battery state of charge

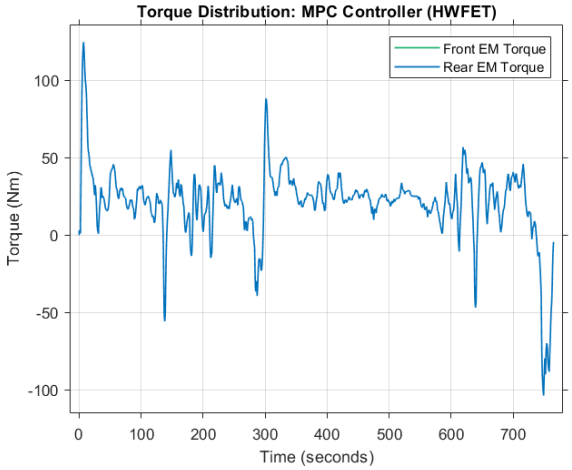

(c) Torque distribution

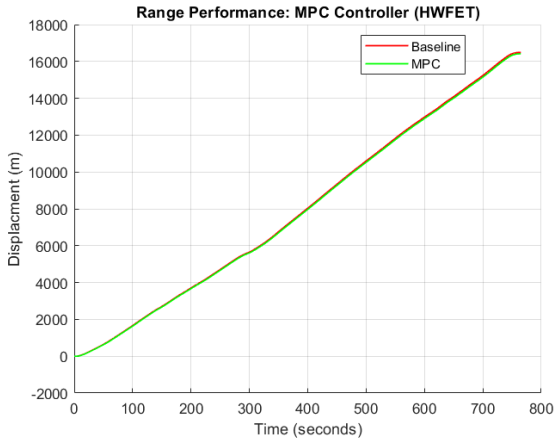

(d) Range of travel

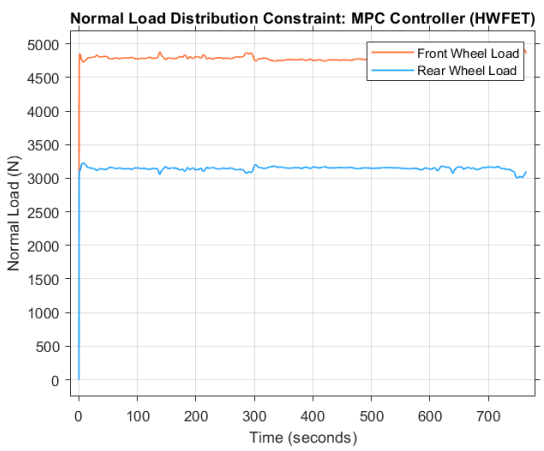

(e) Wheel Normal load

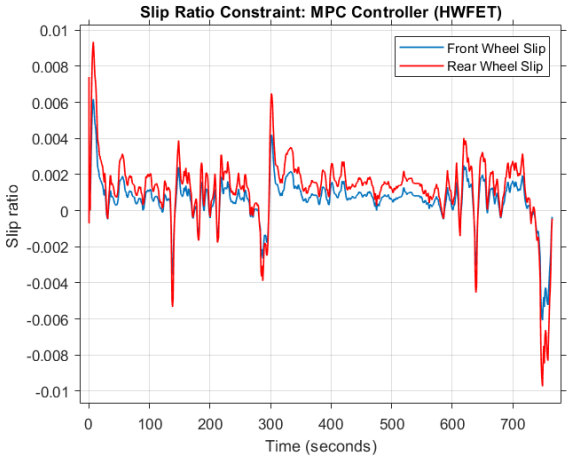

(f) Wheel slip ratio

Figure 12: MPC controller performance on HWFET Drive Cycle (a-f)

5.5.3 FTP75 Drive Cycle

The tracking performance on the FTP75 drive cycle compared to the baseline controller results and total energy consumption in percentage battery state of charge of the MPC controller is shown in table below. Figure 13 (e) and (f) also shows that the constraint on the slip ratio and normal load on each wheel were not violated.

MPC controller tracking offset compared to baseline and total energy consumption for FTP75 Drive Cycle

Tracking/Range offset (%)	Energy consumption (%BSOC)
-0.4438	2.2808

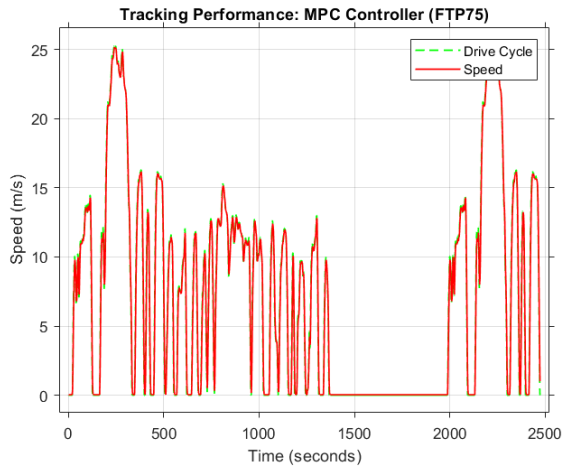

(a) Output tracking

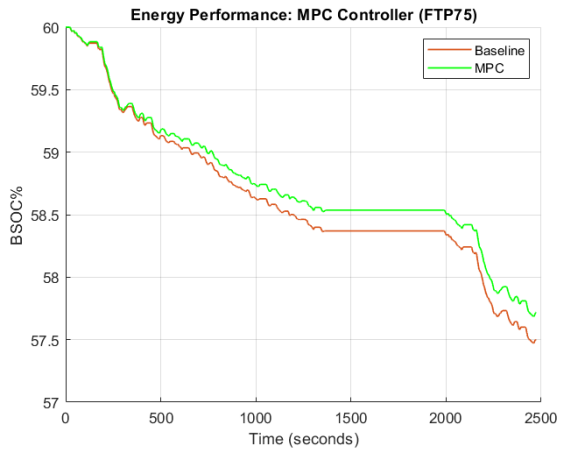

(b) Battery state of charge

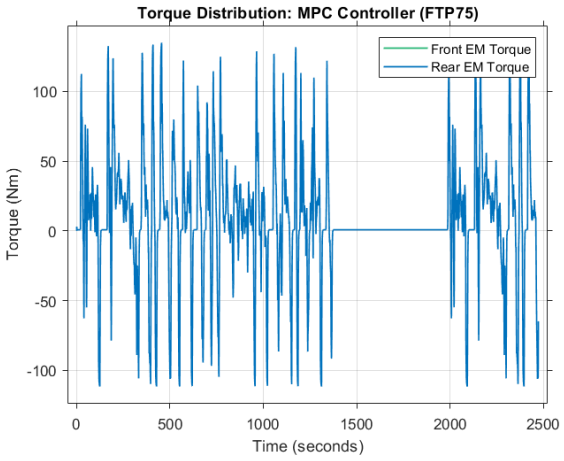

(c) Torque distribution

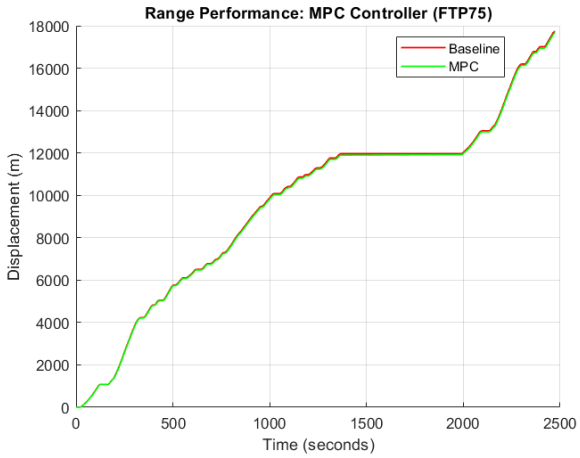

(d) Range of travel

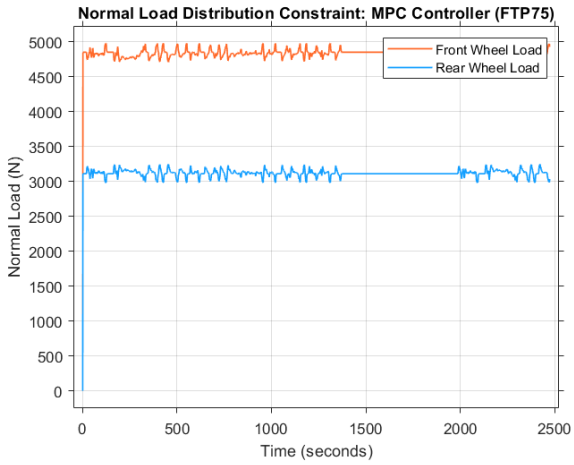

(e) Wheel Normal load

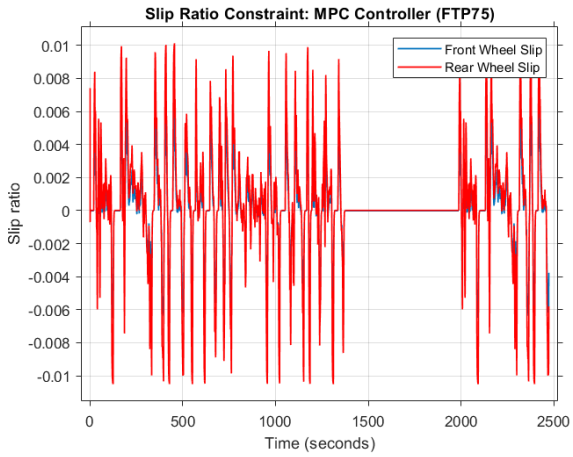

(f) Wheel slip ratio

Figure 13: MPC controller performance on FTP75 Drive Cycle (a-f)

5.5.4 US06 Drive Cycle

The tracking performance compared to the baseline controller results and total energy consumption in percentage battery state of charge of the MPC controller is shown in table below. Figure 14 (e) and (f) also shows that the constraint on the slip ratio and normal load on each wheel were not violated.

MPC controller tracking offset compared to baseline and total energy consumption for US06 Drive Cycle

Tracking/Range offset (%)	Energy consumption (%BSOC)
-0.4166	2.8304

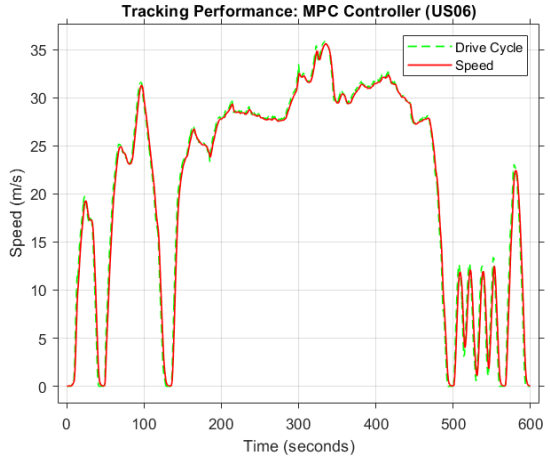

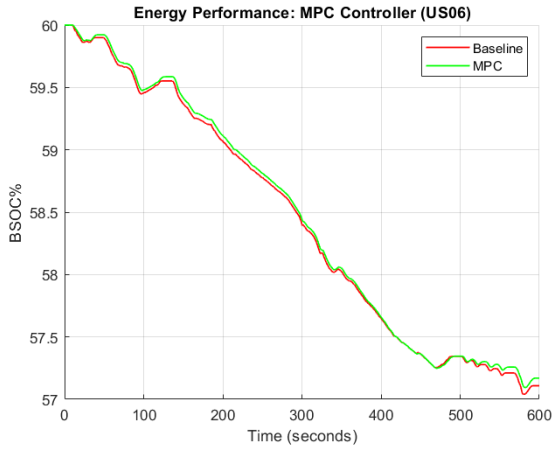

(a) Output tracking

(b) Battery state of charge

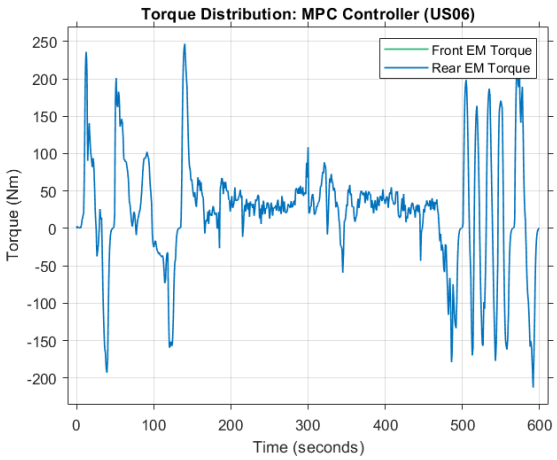

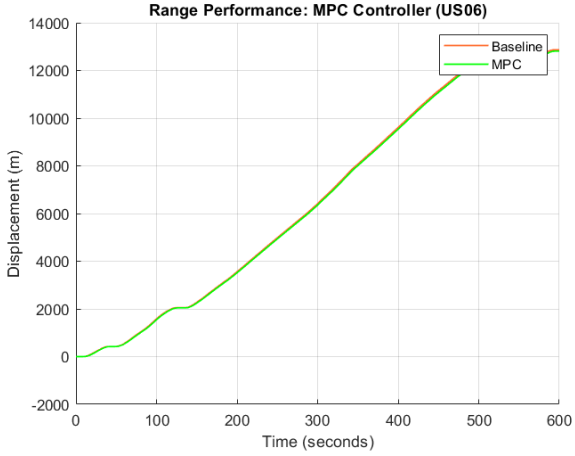

(c) Torque distribution

(d) Range of travel

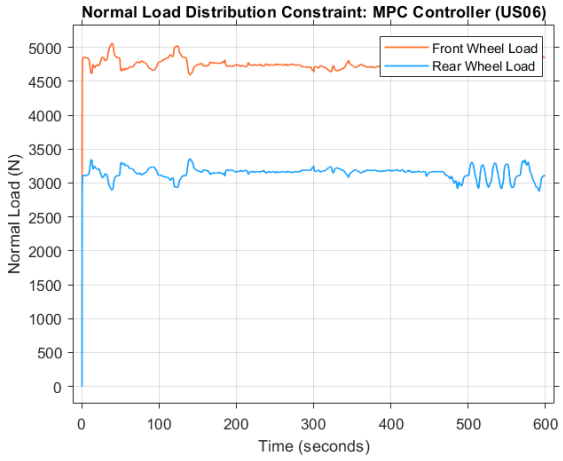

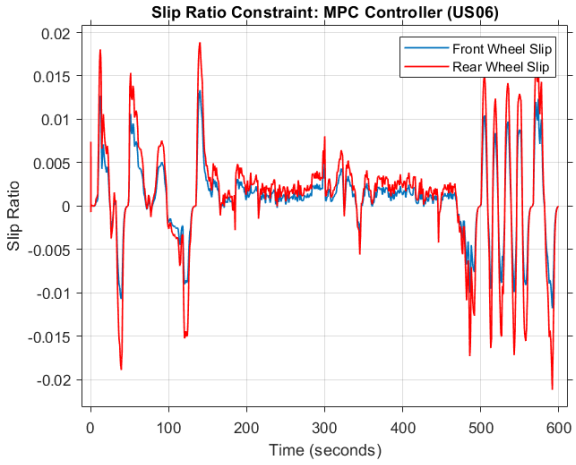

(e) Wheel Normal load

(f) Wheel slip ratio

Figure 14: MPC controller performance on US06 Drive Cycle (a-f)

5.6 MPC + Rule-based Controller Description

In this section, the results showing the performance of the MPC controller plus a rule-based logic, in terms of output tracking, amount of energy used, range covered, and constraints violation will be shown for the WLTP Class 3, HWFET, FTP75 and US06 drive cycles.

The controller output is further processed in this set up. It involves allowing the rear motor to provide all the torque up to a threshold which is 70% of the electric motor capacity. Beyond this threshold, the torque is split equally between the rear and front motors. In the same way, the front wheel supplies the braking torque up to the same threshold and splits the torque equally between the front and rear motors beyond this threshold.

5.7 MPC+Rule-based Controller Performance

5.7.2 WLTP Class 3 Drive Cycle

The tracking performance compared to the baseline controller results and total energy consumption in percentage battery state of charge of the MPC+Rule-Based controller is shown in table below. Figure 15 (e) and (f) also show that the constraint on the slip ratio and normal load on each wheel were not violated.

MPC+Rule-Based controller tracking offset compared to baseline and total energy consumption for WLTP Class 3 Drive Cycle

Tracking/Range offset (%)	Energy consumption (%BSOC)
-0.2256	3.8609

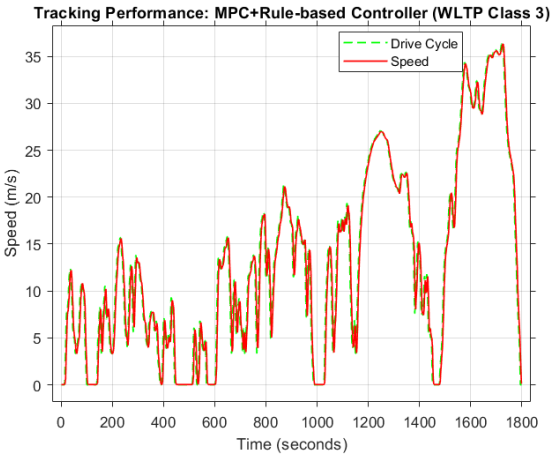

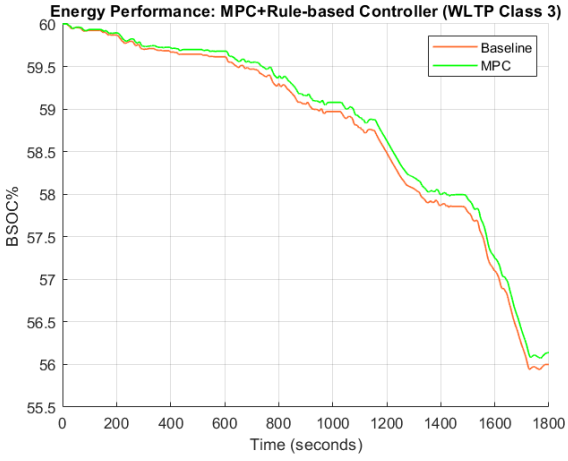

(a) Output tracking

(b) Battery state of charge

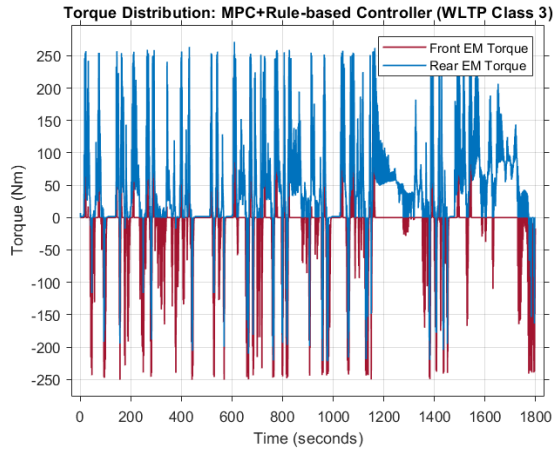

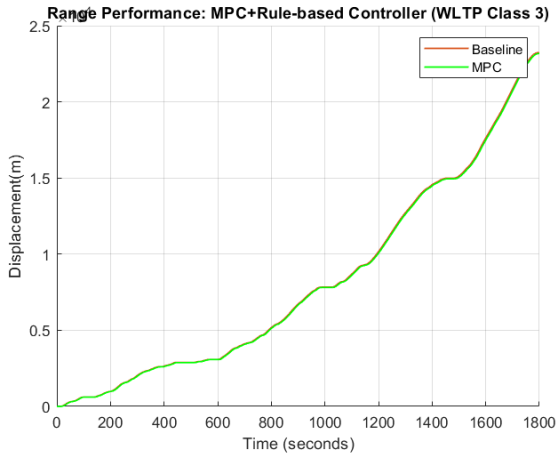

(c) Torque distribution

(d) Range of travel

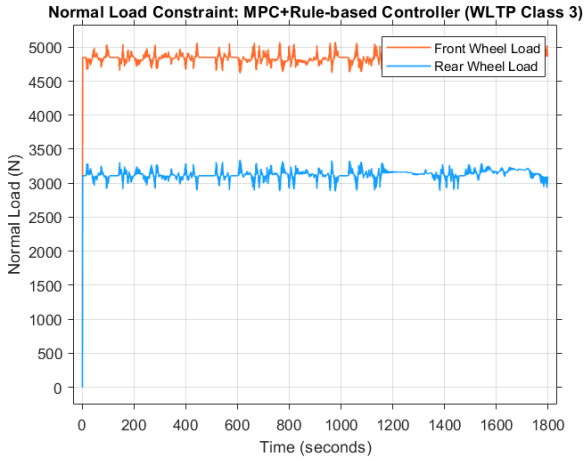

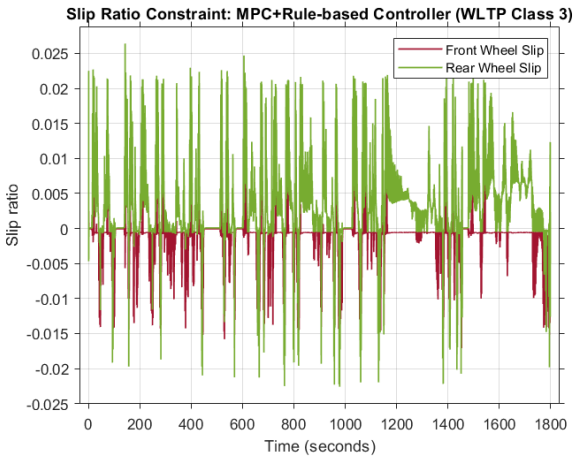

(e) Wheel Normal load

(f) Wheel slip ratio

Figure 15: MPC+Rule-based controller performance on WLTP Class 3 Drive Cycle (a-f)

5.7.3 HWFET Drive Cycle

The tracking performance compared to the baseline controller results and total energy consumption in percentage battery state of charge of the MPC+Rule-Based controller is shown in the table below. Figure 16 (e) and (f) also show that the constraint on the slip ratio and normal load on each wheel were not violated.

MPC+Rule-Based controller tracking offset compared to baseline and total energy consumption for HWFET Drive Cycle

Tracking/Range offset (%)	Energy consumption (%BSOC)
-0.1977	2.5757

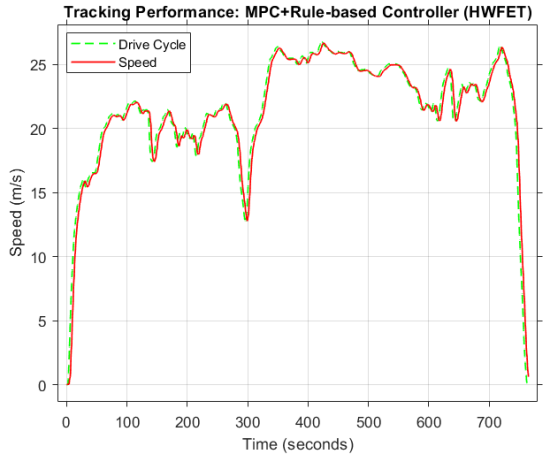

(a) Output tracking

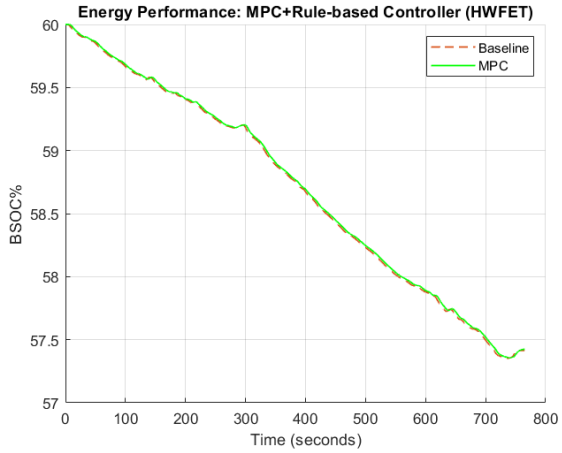

(b) Battery state of charge

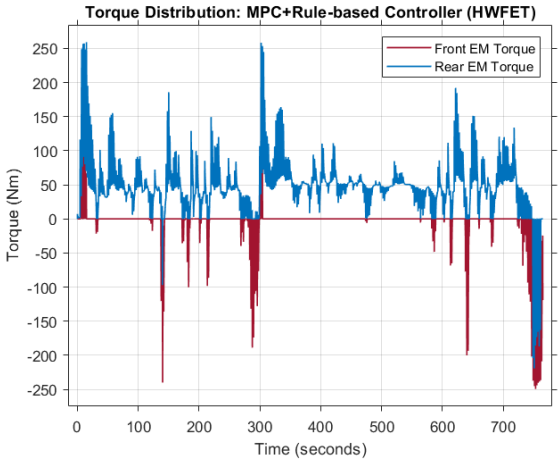

(c) Torque distribution

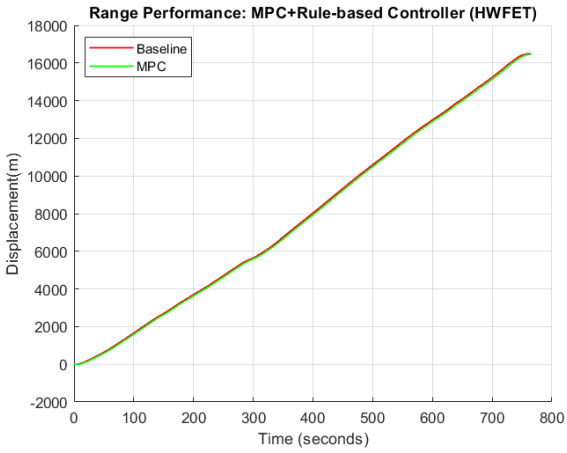

(d) Range of travel

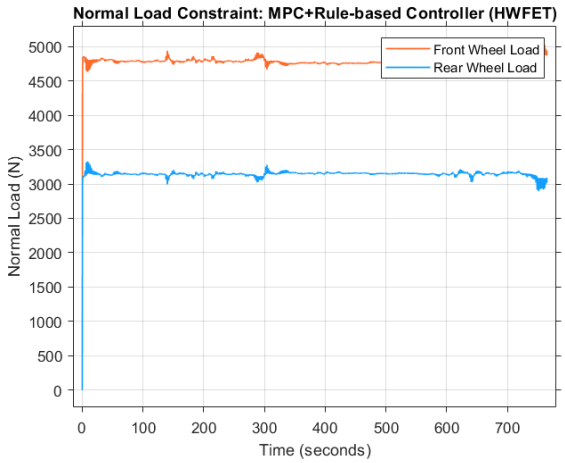

(e) Wheel Normal load

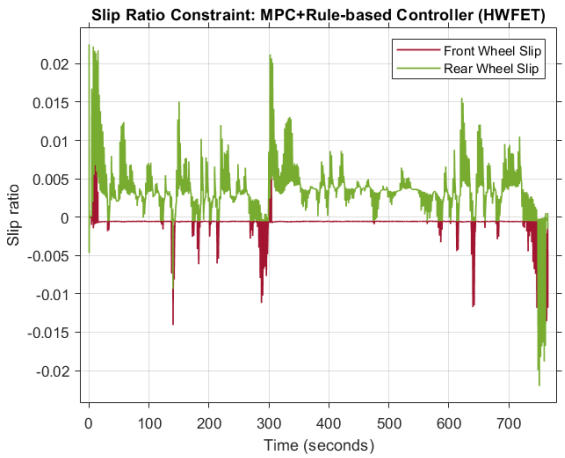

(f) Wheel slip ratio

Figure 16:MPC+Rule-based controller performance on HWFET Drive Cycle (a-f)

5.7.4 FTP75 Drive Cycle

The tracking performance compared to the baseline controller results and total energy consumption in percentage battery state of charge of the MPC+Rule-Based controller is shown in the table below. Figure 17 (e) and (f) also show that the constraint on the slip ratio and normal load on each wheel were not violated.

MPC+Rule-Based controller tracking offset compared to baseline and total energy consumption for FTP75 Drive Cycle

Tracking/Range offset (%)	Energy consumption (%BSOC)
-0.1461	2.2757

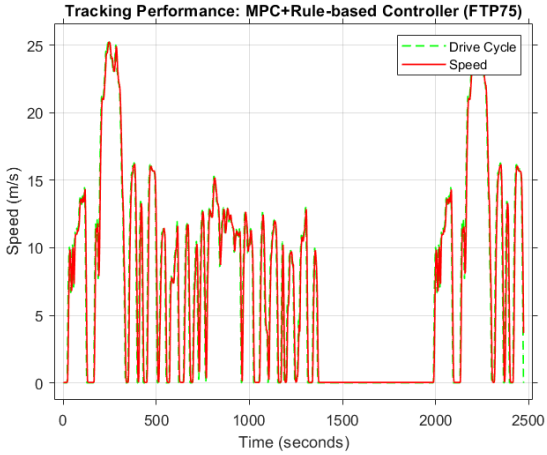

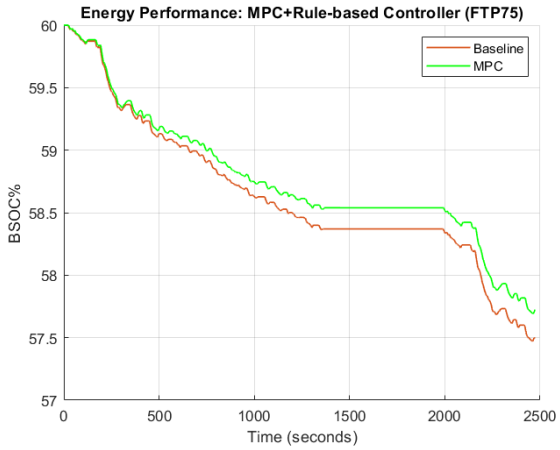

(a) Output tracking

(b) Battery state of charge

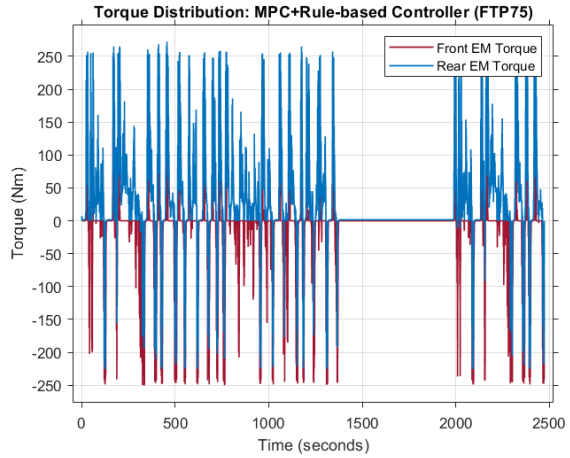

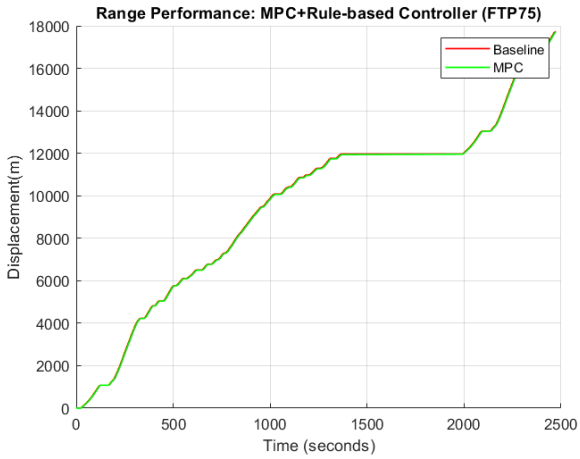

(c) Torque distribution

(d) Range of travel

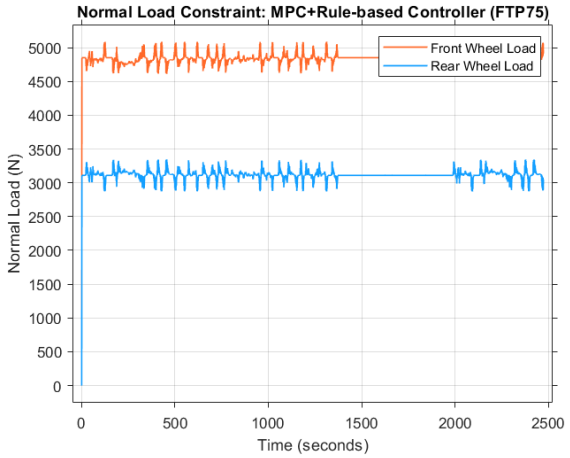

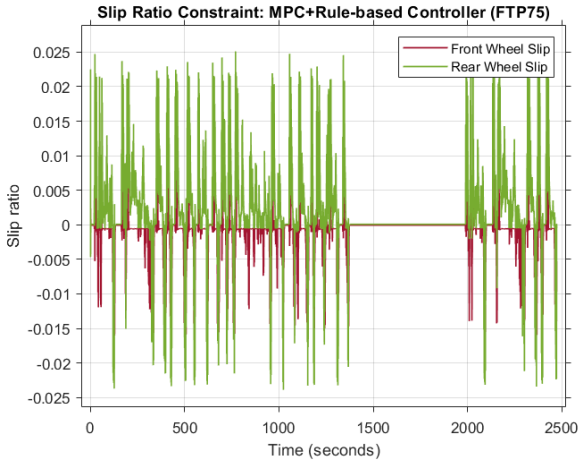

(e) Wheel Normal load

(f) Wheel slip ratio

Figure 17: MPC+Rule-based controller performance on FTP75 Drive Cycle (a-f)

5.7.5 US06 Drive Cycle

The tracking performance compared to the baseline controller results and total energy consumption in percentage battery state of charge of the MPC+Rule-Based controller is shown in the table below. Figure 18 (e) and (f) also show that the constraint on the slip ratio and normal load on each wheel were not violated.

MPC+Rule-Based controller tracking offset compared to baseline and total energy consumption for US06 Drive Cycle

Tracking/Range offset (%)	Energy consumption (%BSOC)
-0.1648	2.7841

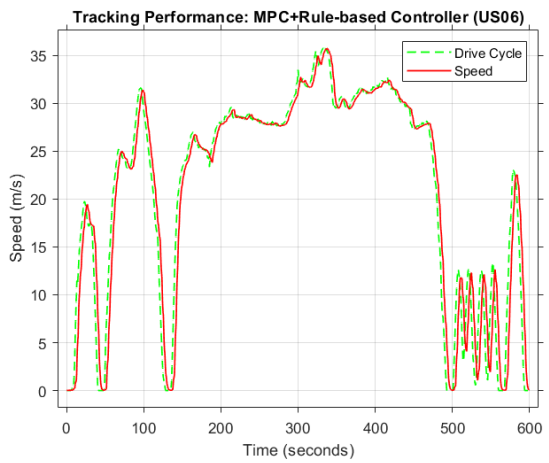

(a) Output tracking

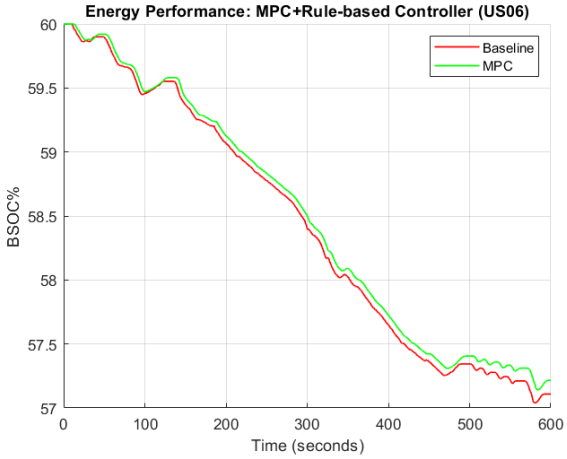

(b) Battery state of charge

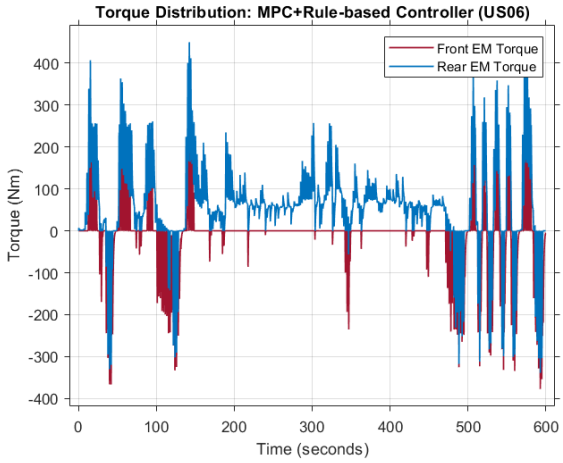

(c) Torque distribution

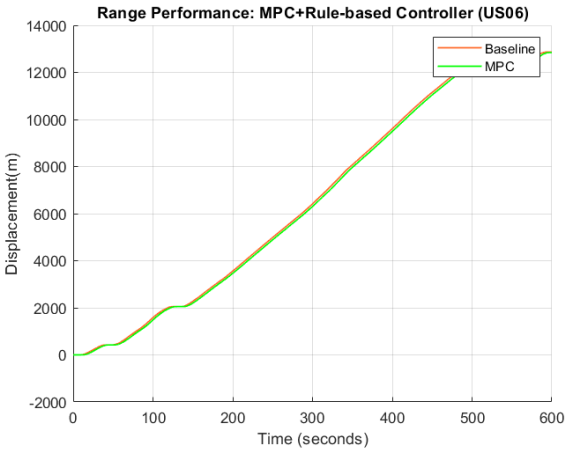

(d) Range of travel

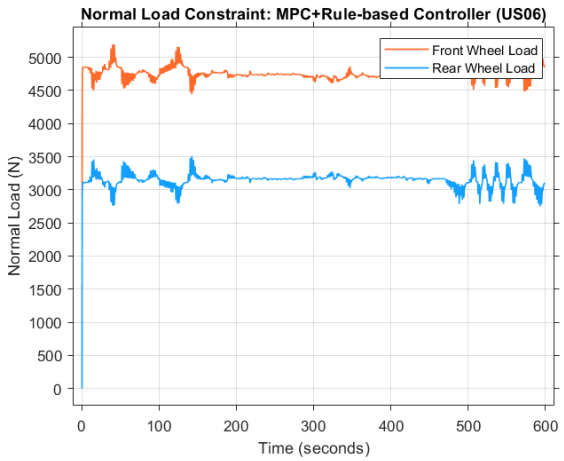

(e) Wheel Normal load

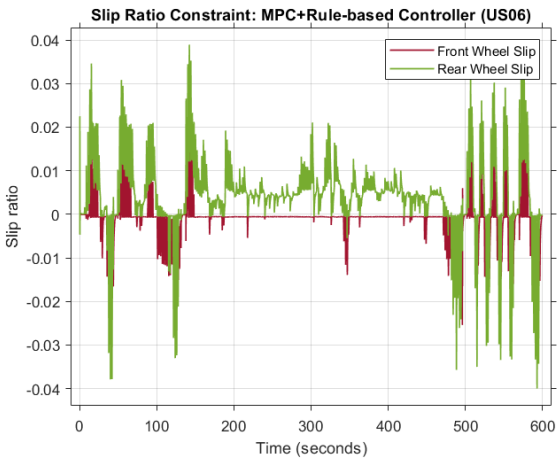

(f) Wheel slip ratio

Figure 18: MPC+Rule-based controller performance on US06 Drive Cycle (a-f)

6

CHAPTER SIX: ANALYSIS OF RESULTS

This section analyses the results extracted in chapter five in terms of energy performance compared to the baseline controller for both the MPC controller and the MPC+Rule-based controller from simulation on each of the drive cycle above.

The energy saved is adjusted by adding the range offset to the total savings to account for the range difference by the different controllers.

6.1 MPC Controller Results Analysis

Table 6: Energy performance of MPC controller compared to Baseline Controller

Drive Cycle	Energy saved (%)	Tracking/Range offset (%)	Adjusted Energy saved (%)
WLTP Class 3	1.65	-0.53	1.12
HWFET	-0.91	-0.45	-1.35
FTP75	8.80	-0.44	8.36
US06	2.11	-0.42	1.70

Figure 19: Chart 1- MPC Controller Performance compared to Baseline Controller Performance

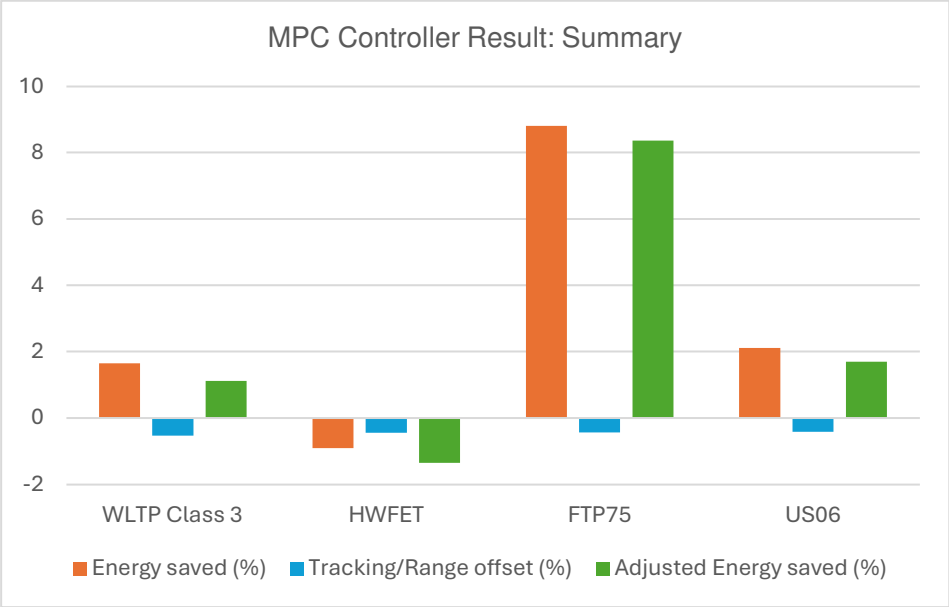

Chart 1 shows that the largest energy savings was gotten from the FTP75 drive cycle and the there were energy losses in the HWFET highway drive cycles. As already mentioned, there was considerable offset in the range compared to the baseline controller as shown in table 6 above.

6.2 MPC+Rule-based Controller Result Analysis

Table 7: Energy performance of MPC+Rule-based controller compared to Baseline Controller

Drive Cycle	Energy saved (%)	Tracking/Range offset (%)	Adjusted Energy saved (%)
WLTP Class 3	3.48	-0.23	3.25
HWFET	0.38	-0.20	0.18
FTP75	9.01	-0.15	8.86
US06	3.71	-0.16	3.55

Figure 20: Chart 2: +Rule-based Controller Performance compared to Baseline Controller Performance

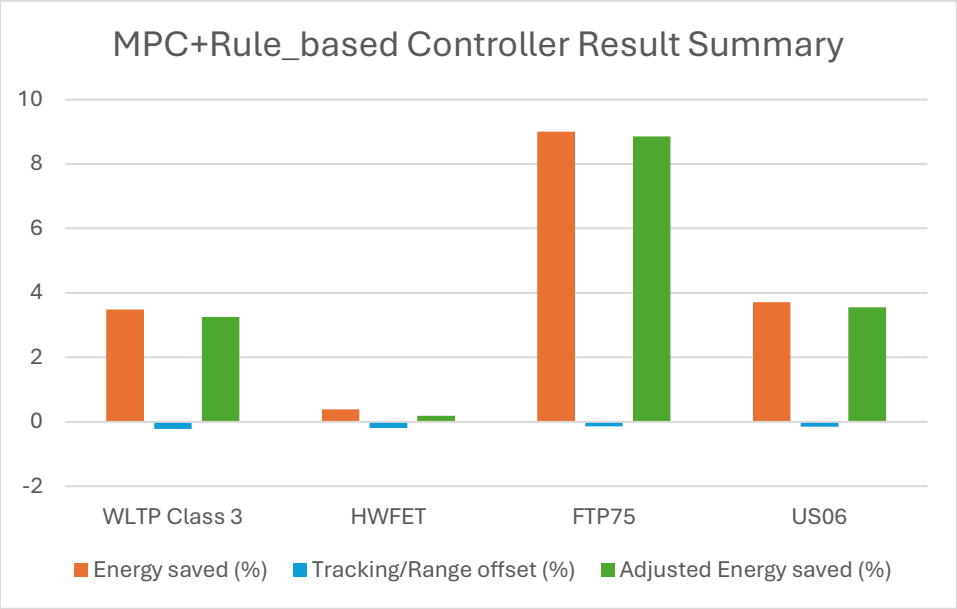

Chart 2 shows that the performance of the MPC controller can be further improved by incorporating the rule-based logic after the MPC controller. This led to a further increase in percentage savings for all the drive cycles. The highway drive cycle improved from -1.35 to 0.18% improvement in efficiency. While energy performance doubled in the US06 and WLTP drive cycles but it only marginally increased in the FTP75 drive cycle.

Figure 21: Chart 3: Energy Savings by each control strategy compared to the baseline

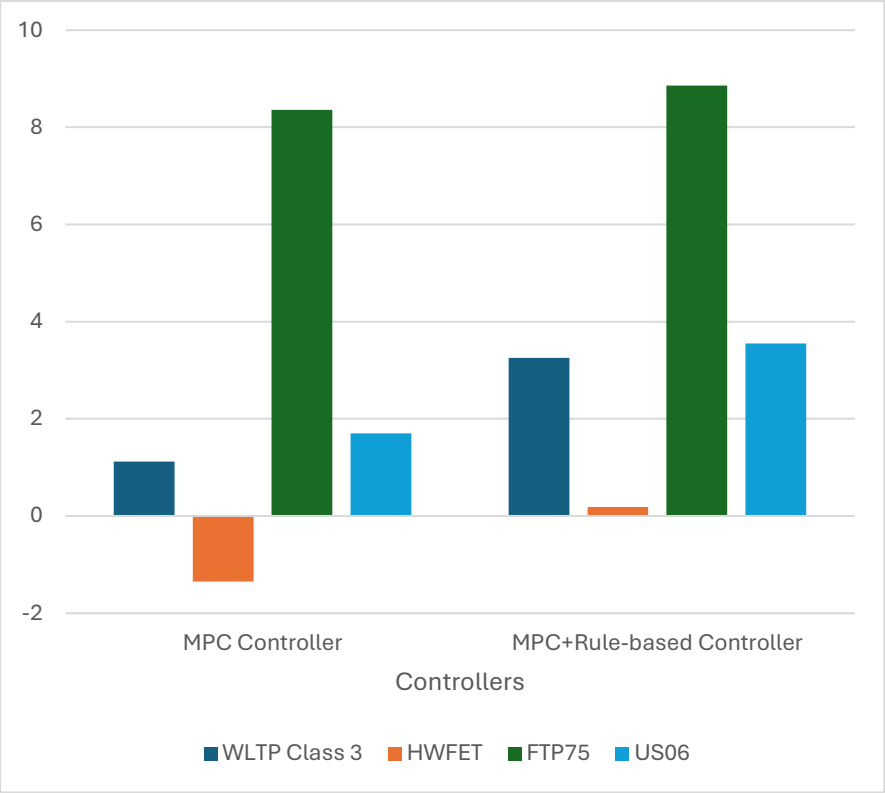

6.3 Energy Performance of all Drive Cycles

Below is the energy performance of all the drive cycles for the baseline, MPC and MPC+Rule-based controller.

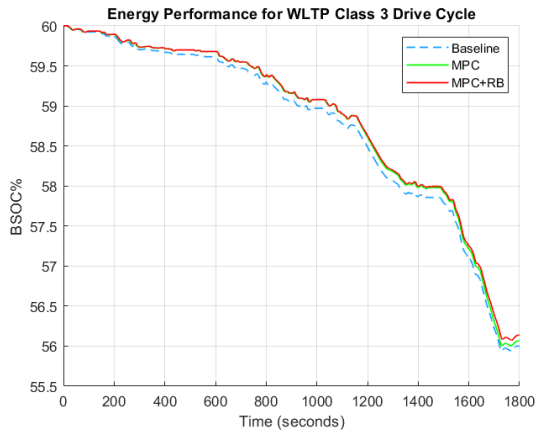

(a) WLTP Drive Cycle

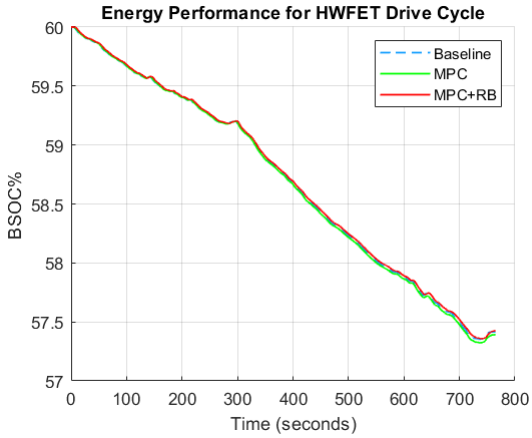

(b) HWFET Drive Cycle

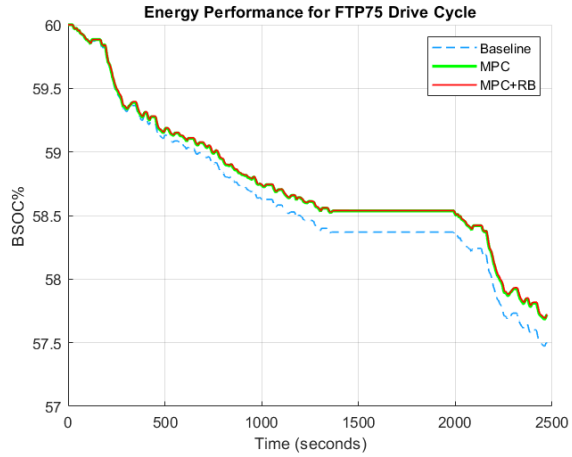

(c) FTP75 Drive Cycle

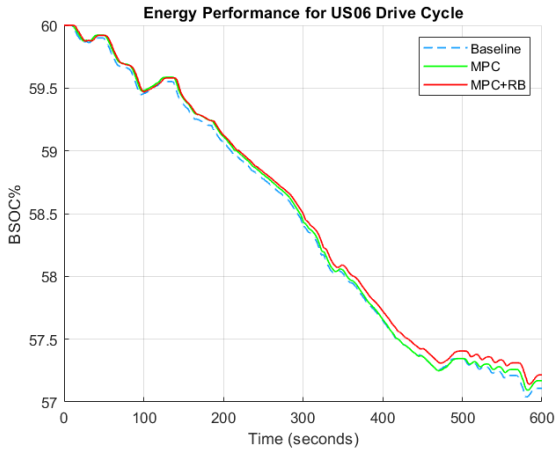

(d) US06 Drive Cycle

Figure 22: Energy Performance baseline, MPC and MPC+Rule-based Controllers in terms of battery state of charge

6.4 Summary of Energy Efficiency Improvements

Chart 4 provides a summary of the energy performance improvements achieved by both the MPC controller and the MPC+Rule-based controller in miles per gallon equivalent (MPGe). Overall, the MPC+Rule-based controller further improved the gains of the MPC controller alone.

The table below shows the summary of the performance of the controllers in Mile per gallons equivalent (MPGe)

Table 8: Efficiency improvement by the controllers in MPGe

Drive Cycle	MPC	MPC+RB
WLTP	2.522573	4.3704745
HWFET	-0.56637	0.7250277
FTP75	14.11502	14.00053
US06	2.258203	3.518235

Figure 23: Chart 4: Efficiency Improvements in Miles per Gallon Equivalent (MPGe)

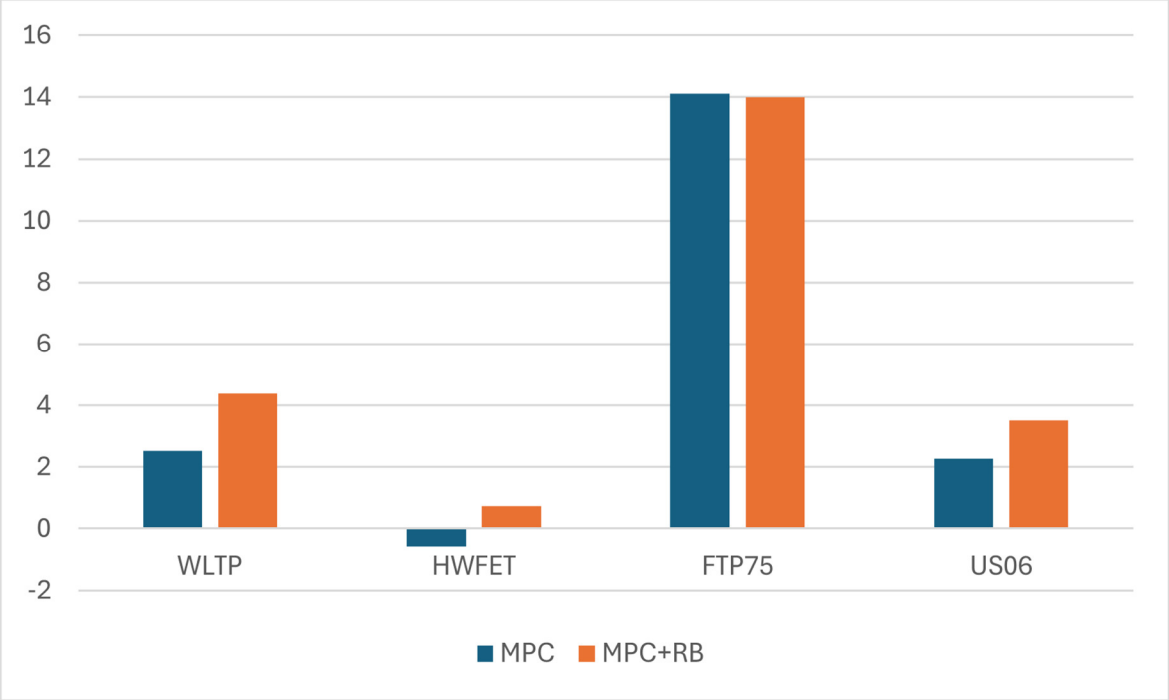

7

CHAPTER SEVEN: CONCLUSION

Contents

7.1 Conclusion

The results and analysis of the results from chapter 5 and 6 shows that the more complex a drive cycle, the more opportunity to save energy using the model predictive controller. While urban and more aggressive city drive cycles (WLTP, FTP75 and US06) resulted in considerable energy savings, highway drive cycles with relatively constant speed (HWFET) and little to no stops resulted in losses or low energy improvements. This is not surprising because the speed and battery state of charge are the system states in the MPC prediction model. Hence, the MPC algorithm tends to better optimize when the variations in states are frequent. This implies that it will be difficult to further optimize the drivetrain based on parameters like speed and state of charge. One may need to consider more intrinsic properties of the system such as efficiency, battery current, voltage, motor losses etc.

One clear observation is the opposing nature of speed tracking and energy optimization. Where energy performance leads to savings, tracking is usually sacrificed. This means that control designers must clearly define acceptable and unacceptable tracking performance. It is important not just for the speed to be adequately tracked but for the controller to do it at a very fast rate. Anything less will lead to poor response time which may be detrimental for

more aggressive driving conditions. It is worth noting that even though the rule-based approach improved the tracking and energy performance, it added a perhaps unwanted delay of about 1 second to the control response time. At this junction, the author would like to point out that this demerit of the inclusion of rule-based component will require delving deeper into to properly understand and quantify the impact of this approach to system response, stability, driving comfort etc.

In Conclusion, MPC as a strategy can optimize the efficiency of current IDA DM-BEV powertrain in urban settings. However, it is less likely to do the same for highway drive cycles with the current problem formulation. However, an MPC plus rule-based strategy can further improve the efficiency of the IDA BM-BEV drive trains compared to MPC in both urban and highway settings.

7.2 Future Work

Future works could focus on integrating the driving mode/rule-based logic into control algorithm to further improve energy performance. This is justified because the rule-based implementation of the torque split at a fix threshold is often suboptimal especially when one considers very uncertain terrains. The optimal torque split threshold may vary for different road conditions. Designing an MPC algorithm which considers all these conditions is still a subject for further research. Hence future studies could involve incorporating the rule-based logic as a nonlinear constraint in the MPC structure.

Secondly, more detailed modelling which considers the wheel, battery and motor dynamics could further improve efficiency. Using neural network models to approximate some highly nonlinear components of the powertrain such as the wheel dynamics which incorporates the so called Pacejka formula could further simplify the modeling approaches and makes it possible to control highly nonlinear dynamics efficiently.

Another area of possible development is the use of velocity based linear parameter approximation of the nonlinear system with known and unknown drive cycle. stability issues which arise because of the quasi LPV structure of the model. Finally, Future research or implementation could focus on how to further reduce the computational burden by adopting

the velocity based LPV approximation of the system and avoid issues of instability caused by switching control operating points from one equilibrium point to another.

One largely unexplored area will be in the use of reinforcement learning based approaches which have been shown to be more adaptable to unknown drive cycles and result in relatively more optimal solutions. They are often not dependent on the powertrain dynamics hence simplifying the modeling approach used for the deriving the prediction model(A. Biswas, P. G. Anselma & A. Emadi, 2022).

Finally, to handle highly nonlinear constraints imposed by the driving mode selection, the general recommendation is the use of more application specific solvers suitable for automotive application to better deal with these constraints and hence result in optimal solutions.

APPENDIX

A. SIMULINK FILES

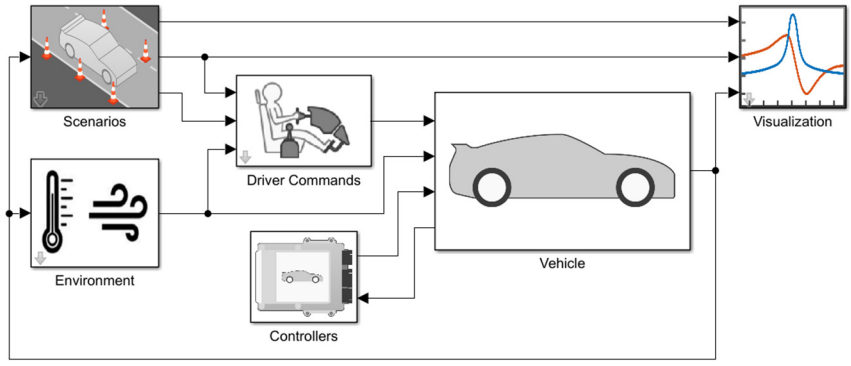

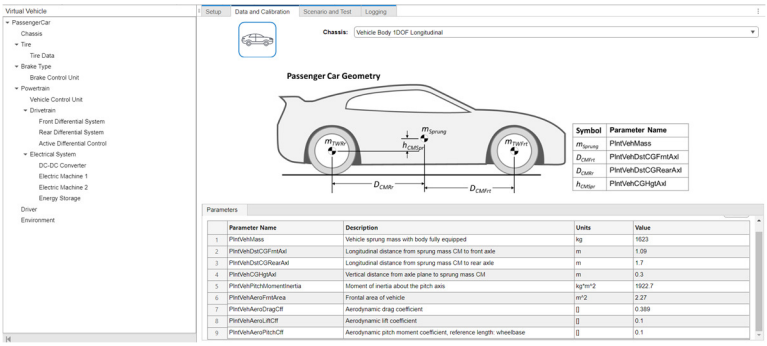

Figure a: “Electric 2EM Vehicle” Reference Application

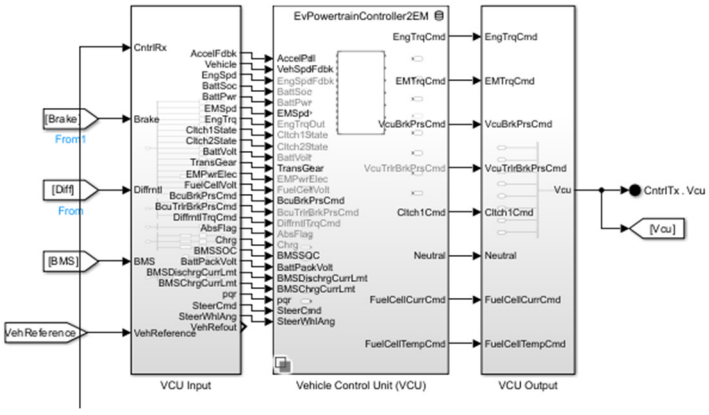

Figure b: Electric 2EM Vehicle Control Unit

APPENDIX

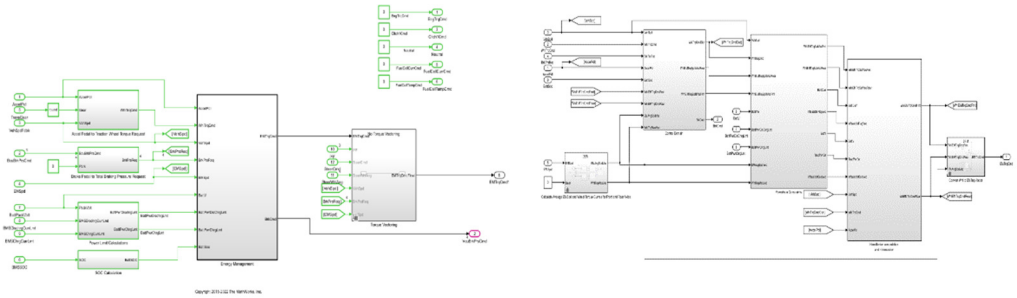

i. Overview ii. Internal look at Energy Management block

Figure c: Baseline Controller Set up

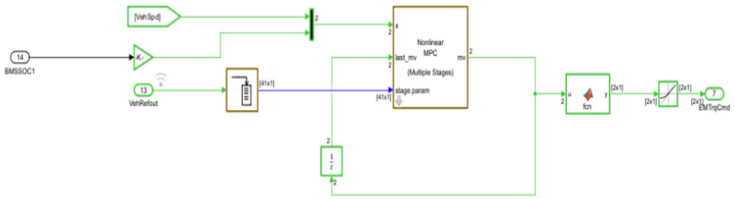

Figure d: MPC+RB Controller Set up

B. CALCULATION SHEETS

Conversion from Battery State of Charge to Mile per Gallon Equivalent (MPGe)

				meters	mile
Capacity of Battery(kWh)	106.69752		Distance	23228	14.43325
Meters-Miles Conversion Factor	1609.34			MPC	MPC+RB
			Range offset	-0.5291	-0.2259
WLTP Drive Cycle					
	Baseline	MPC	MPC+RB		
TSOC Range	56.0001	56.0659	56.1391		
energy consumed(kWh)	4.267794102	4.197587	4.119485		
MPGe	113.9699751	115.8762	118.0731		
Adjusted MPGe based on Range offset		116.4925	118.3404		
		2.522573	4.370475		

				meters	mile
Capacity of Battery(kWh)	106.69752		Distance	16487.3	10.24476
Meters-Miles Conversion Factor	1609.34			MPC	MPC+RB
			Range offset	-0.4464	-0.1977

HWFET

	Baseline	MPC	MPC+RB
TSOC Range	57.4145	57.3911	57.4243
energy consumed(kWh)	2.75866438	2.783632	2.748208
MPGe	125.1505516	124.028	125.6267
Adjusted MPGe		124.5842	125.8756
		-0.56637	0.725028

				meters	mile
Capacity of Battery(kWh)	106.69752		Distance	17733.2	11.01893
Meters-Miles Conversion Factor	1609.34			MPC	MPC+RB
			Range offset	-0.4438	-0.1461

FTP75

	Baseline	MPC	MPC+RB
TSOC Range	57.499	57.7192	57.7243
energy consumed(kWh)	2.668504975	2.433557	2.428115
MPGe	139.1557609	152.5906	152.9325
Adjusted MPGe		153.2708	153.1563
		14.11502	14.00053

				meters	mile
Capacity of Battery(kWh)	106.69752		Distance	12865.2	7.994085
Meters-Miles Conversion Factor	1609.34			MPC	MPC+RB

			Range Offset	-0.4166	-0.1648
US06					
	Baseline	MPC	MPC+RB		
TSOC Range	57.1085	57.1696	57.2159		
energy consumed(kWh)	3.085158791	3.019967	2.970566		
MPGe	87.32148553	89.2065	90.69002		
Adjusted MPGe		89.57969	90.83972		
		2.258203	3.518235		

BIBLIOGRAPHY

References

1. A. Biswas, P. G. Anselma & A. Emadi. (2022) Real-Time Optimal Energy Management of Multimode Hybrid Electric Powertrain With Online Trainable Asynchronous Advantage Actor–Critic Algorithm. *IEEE Transactions on Transportation Electrification.* 8 (2), 2676–2694. 10.1109/TTE.2021.3138330.

2. Angeli, D. (2012) Lecture Notes Stability and Control of Nonlinear Systems.

3. Cavanini, L., Majecki, P., Grimble, M. J., Sasikumar, L. V., Li, R. & Hillier, C. (2022) *Processor-In-the-Loop Demonstration of MPC for HEVs Energy Management System.* Elsevier BV.

4. Grimble, M. J. & Majecki, P. (2020) *Nonlinear Industrial Control Systems Optimal Polynomial Systems and State-Space Approach.* 1st edition. London, Springer London.

5. He, Z., Shi, Q., Wei, Y., Zheng, J., Gao, B. & He, L. (2021) A Torque Demand Model Predictive Control Approach for Driving Energy Optimization of Battery Electric Vehicle. *IEEE Transactions on Vehicular Technology.* 70 (4), 3232–3242. 10.1109/TVT.2021.3066405.

6. Huang, Y., Wang, H., Khajepour, A., He, H. & Ji, J. (2016) Model predictive control power management strategies for HEVs: A review. *Journal of Power Sources.* 341 91. 10.1016/j.jpowsour.2016.11.106.

7. Illinois Institute of Technology. (nd) *Stiffness and Stability.* http://www.math.iit.edu/~fass/478578_Chapter_4.pdf [Accessed 27th August, 2024].

8. Karthika & Padmasuresh:. (2022) A Review on Optimal Energy Management Strategies for Electric Vehicles. *2022 Third International Conference on Intelligent Computing Instrumentation and Control Technologies (ICICICT).* , IEEE.

9. *Electric Vehicles: The Future of Development and Deployment.* (2019) Directed by: S. Ladislaw, N. Albanese, G. Fitzgerald & J. Meckling.

10. Louback, E., Biswas, A., Machado, F. & Emadi, A. (2024) A review of the design process of energy management systems for dual-motor battery electric vehicles. *Renewable and Sustainable Energy Reviews.* 193 10.1016/j.rser.2024.114293.

11. MathWorks. (2024b) *Matlab Simulink Challenge Project Hub.* https://github.com/mathworks/MATLAB-Simulink-Challenge-Project-Hub/tree/main/projects/Energy%20Management%20for%20a%202-Motor%20BEV%20using%20Model-Predictive%20Control [Accessed 1 March, 2024].

12. MathWorks. (2024c) *Model Predictive Control Toolbox: Nonlinear MPC design.* https://uk.mathworks.com/help/mpc/nonlinear-mpc-design.html [Accessed 7th, September, 2024].

13. MathWorks. (2024a) *Multistage Nonlinear Model Predictive Controller.* https://uk.mathworks.com/help/mpc/ref/nlmpcmultistage.html?searchHighlight=implicit%20euler%20multistage%20nonlinear%20mpc&s_tid=srchtitle_support_results_1_implicit%2520euler%2520multistage%2520nonlinear%2520mpc [Accessed 27th, August, 2024a].

14. MathWorks. (2023b) *PowerTrain Blockset Reference Guide.*

15. MathWorks. (2023a) *PowerTrain User Guide.* MathWorks.

16. MathWorks. (2022) *Virtual Vehicle Composer* (2023b) .

17. Musardo, C., Rizzoni, G., Guezennec, Y. & Staccia, B. (2005) A-ECMS: An Adaptive Algorithm for Hybrid Electric Vehicle Energy Management. *European Journal of Control.* 11 (4-5), 509–524. 10.3166/ejc.11.509-524.

18. *Overview of Electric Vehicles in India.* (2020) Directed by: NPTEL-NOC IIT Madras.

19. Rajamani, R. (2012) *Vehicle dynamics and control.* 2nd edition. New York ;, Springer.

20. Rawlings et al. (2022) *Model Predictive Control: Theory, Computation and Design.* Santa Barbara California, Nob Hill Publishing, LLC.

21. Schwenzer, M., Ay, M., Bergs, T. & Abel, D. (2021) Review on model predictive control: an engineering perspective. *The International Journal of Advanced Manufacturing Technology.* 117 (5-6), 1327. 10.1007/s00170-021-07682-3.

22. Thomas, P. (1999) *Simulation of industrial processes for control engineers.* Oxford ;, Butterworth-Heinemann.

23. Wang, Z., Zhou, J. & Rizzoni, G. (2022) *A review of architectures and control strategies of dual-motor coupling powertrain systems for battery electric vehicles.* Elsevier BV.

24. Yang, B., Guo, L., Ye, J. & Velni, J. M. (2021) Energy Management Strategy for Dual-Motor-Based Electric Vehicle Powertrain Using Nonlinear Model Predictive Control. *2021 IEEE Transportation Electrification Conference & Expo (ITEC).* , IEEE.

25. Zheng, Q., Tian, S. & Zhang, Q. (2020) Optimal Torque Split Strategy of Dual-Motor Electric Vehicle Using Adaptive Nonlinear Particle Swarm Optimization. *Mathematical Problems in Engineering.* 2020 1–21. 10.1155/2020/1204260.